

Flavor Asymmetry of Light Quarks in the Nucleon Sea

Gerald T. Garvey and Jen-Chieh Peng
Physics Division
Los Alamos National Laboratory
Los Alamos, New Mexico, 87545 USA

November 2, 2018

Abstract

A surprisingly large asymmetry between the up and down sea quark distributions in the nucleon has been observed in recent deep inelastic scattering and Drell-Yan experiments. This result strongly suggests that the mesonic degrees of freedom play an important role in the description of the parton distributions of the hadronic sea. In this article, we review the current status of our knowledge of the flavor structure of the nucleon sea. The implications of various theoretical models as well as possible future measurements are also discussed.

1 Introduction

The first direct evidence for point-like constituents in the nucleons came from the observation of scaling phenomenon in Deep-Inelastic Scattering (DIS) experiments [1, 2] at SLAC. These point-like charged constituents, called partons, were found to be spin-1/2 fermions. These partons were initially identified as the quarks in the Constituent Quark Models (CQM). However, it was soon realized that valence quarks alone could not account for the large enhancement of the cross sections at small Bjorken- x , the fraction of nucleon momentum carried by the partons. This swarm of low-momentum partons, dubbed wee-partons by Feynman [3], was interpreted as the quark and antiquark sea of the nucleon. DIS experiments therefore provided the first evidence for the existence of antiquarks in the nucleon.

The observation of partons in DIS experiments paved the road to the formulation of Quantum Chromodynamics (QCD) as the theory for strong interactions. Nevertheless, the exact form of the parton distribution functions (PDF) can not be deduced from perturbative QCD. Like many other static properties of hadrons, the parton distribution functions belong to the domain of non-perturbative QCD. In spite of great progress [4] made in Lattice Gauge Theory (LGT) in treating the bound-state properties of hadrons, it remains a challenge to predict the parton distributions using LGT.

Until parton distributions can be readily calculated from first principles, they are best determined from experiments. Electroweak processes such as DIS and lepton-pair production provide the cleanest means to extract information on the parton distributions. There are at least two reasons why it is important to measure the parton distribution functions. First, the description of hard processes in high energy interactions requires parton distribution functions as an essential input. Second, many aspects of the parton distributions, such as sum rules, scaling-violation, asymptotic behaviors at large and small x , and flavor and spin structures, can be compared with the predictions of perturbative as well as non-perturbative QCD.

In this article, we review the status of our current knowledge of the flavor dependence of the sea quark distributions in hadrons. The recent observation of a striking flavor asymmetry of the nucleon

sea has profound implications on the importance of meson degrees of freedom for the description of parton substructures in the nucleon. In Section 2, we review the early studies of the nucleon sea in DIS and lepton-pair production. The crucial recent experiments establishing the up/down flavor asymmetry of the nucleon sea are discussed in Section 3. The various theoretical models for explaining the flavor asymmetry of the nucleon sea are described in Section 4. The implications of these models on other aspects of the parton structure functions are discussed in Section 5. Finally, we present future prospects in Section 6, followed by the conclusion in Section 7.

2 Early Studies of the Nucleon Sea

2.1 Deep Inelastic Scattering

Although scaling behavior in inelastic electron scattering was predicted by Bjorken [5], based on the framework of current algebra, its confirmation by the SLAC experiments still came as a major surprise. A simple and intuitive picture for explaining the scaling behavior is the parton model advanced by Feynman [3, 6]. In this model, the electron-nucleon deep-inelastic scattering is described as an incoherent sum of elastic electron-parton scattering. However, the nature of the partons within the nucleon was not specified by Feynman. Some authors [7, 8, 9, 10] speculated that the partons were the ‘bare nucleon’ plus the pion cloud, while others [11, 12, 13] believed they were the quarks introduced by Gell-Mann [14] and Zweig [15]. The latter scenario was strongly supported by the measurement of R , ratio of the longitudinally over transversely polarized photon cross sections, showing the spin-1/2 character of the partons.

Evidence for quark-antiquark sea in the nucleon came from the observation that the structure function $F_2(x)$ approaches a constant value as $x \rightarrow 0$ [16]. If the proton is made up of only three quarks, or any finite number of quarks, $F_2(x)$ is expected to vanish as $x \rightarrow 0$. Bjorken and Paschos [11] therefore assumed that the nucleon consists of three quarks in a background of an infinite number of quark-antiquark pairs. Kuti and Weisskopf [12] further included gluons among the constituents of nucleons in order to account for the missing momentum not carried by the quarks and antiquarks alone.

The importance of the quark-antiquark pairs in the nucleon is in sharp contrast to the situation for the atomic system, where particle-antiparticle pairs play a relatively minor role (such as the polarization of the vacuum). In strong interactions, quark-antiquark pairs are readily produced as a result of the relatively large magnitude of the coupling constant α_s , and they form an integral part of the nucleon’s structure.

Neutrino-induced DIS experiments allowed the separation of sea quarks from the valence quarks. Recall that

$$\begin{aligned} F_2^{\nu p}(x) &= 2x \sum_i [q_i(x) + \bar{q}_i(x)], \\ F_3^{\nu p}(x) &= 2 \sum_i [q_i(x) - \bar{q}_i(x)] = 2 \sum_i q_i^v(x), \end{aligned} \tag{1}$$

where i denotes the flavor of the quarks. Note that the valence quark distribution is defined as the difference of the quark and antiquark distributions, $q_i^v(x) = q_i(x) - \bar{q}_i(x)$. Equation 1 shows that the valence quark distribution is simply $F_3^{\nu p}(x)/2$, while the sea quark distribution is given by $F_2^{\nu p}(x)/2x - F_3^{\nu p}(x)/2$. The $F_2^{\nu p}(x)$ and $F_3^{\nu p}(x)$ data from the CDHS experiment [17] clearly showed that the valence quark distributions dominate at $x > 0.2$, while the sea quarks are at small x .

The earliest parton models assumed that the proton sea was flavor symmetric, even though the valence quark distributions are clearly flavor asymmetric. Inherent in this assumption is that the content of the sea is independent of the valence quark’s composition. Therefore, the proton and neutron were expected to have identical sea-quark distributions. The assumption of flavor symmetry was not

based on any known physics, and it remained to be tested by experiments. Neutrino-induced charm production experiments [18, 19], which are sensitive to the $s \rightarrow c$ process, provided strong evidences that the strange-quark content of the nucleon is only about half of the up or down sea quarks. This flavor asymmetry was attributed to the much heavier mass for strange quark compared to the up and down quarks. The mass for the up and down quarks being very similar suggests that the nucleon sea should be nearly up-down symmetric. A direct method to check this assumption is to compare the sea in the neutron to that in the proton by measuring the Gottfried integral in DIS, as discussed next.

2.2 Gottfried Sum Rule

In 1967, Gottfried studied electron-proton scattering with the assumption that the proton consists of three constituent quarks [20]. He showed that the total electron-proton cross section (elastic plus inelastic) is identical to the Rutherford scattering from a point charge. Gottfried derived a sum rule

$$I_2^p = \int_0^1 F_2^p(x, Q^2)/x dx = \sum_i (Q_i^p)^2 = 1, \quad (2)$$

where Q_i^p is the charge of the i th quark in the proton. Gottfried expressed great skepticism that this sum rule would be confirmed by the forthcoming SLAC experiment by stating “*I think Prof. Bjorken and I constructed the sum rules in the hope of destroying the quark model*” [21]. Indeed, Eq. 2 was not confirmed by the experiments, not because of the failure of the quark model, but because of the presence of quark-antiquark sea. In fact, the total number of the sea partons being infinite makes I_2^p diverge. A closely related sum rule, now called the Gottfried Sum Rule (GSR), avoids this problem by considering the difference of the proton and neutron cross sections, namely,

$$I_2^p - I_2^n = \int_0^1 [F_2^p(x, Q^2) - F_2^n(x, Q^2)]/x dx = \sum_i [(Q_i^p)^2 - (Q_i^n)^2] = 1/3. \quad (3)$$

In deriving Eq. 3, it was assumed that the sea quarks in the proton and neutron are identical. Regarding the Gottfried Sum Rule, Kuti and Weisskopf stated in their paper [12] “*This very simple and definite sum rule is based upon our most radical simplification: the assumption that the core carries vacuum quantum numbers so that the isotopic spin of the nucleon is completely carried by the valence quarks*”.

Soon after the discovery of scaling in electron-proton DIS, electron-deuterium scattering experiments were carried out to extract the electron-neutron cross sections. The comparison of $e-p$ with $e-n$ data was very important for distinguishing early competing theoretical models [16]. These data also allowed a first evaluation [22] of the Gottfried integral in 1970. The first result for the Gottfried integral was 0.19, considerably less than 1/3. As the data only covered $x > 0.08$, it was assumed that $F_2^p - F_2^n$ follows Regge behavior (proportional to $x^{1/2}$) in the unmeasured small- x region. Due to the $1/x$ factor in the integrand, the small- x region could have potentially large contributions to the Gottfried integral. Moreover, it was not clear if $F_2^p - F_2^n$ would indeed follow the Regge behavior at small x , and if so, at what value of x would it set in. By 1973, new data were available down to $x = 0.05$ and the Gottfried integral was evaluated to be 0.28 [23], considerably larger than the first result. It should be pointed out that these data were taken at relatively low values of Q^2 . Furthermore, Q^2 varied as a function of x .

Although the large systematic errors associated with the unmeasured small- x region prevented a sensitive test of the GSR, Field and Feynman [24] nevertheless interpreted the early SLAC data as a strong indication that GSR is violated and that the \bar{u} and \bar{d} distributions in the proton are different. The relationship between the Gottfried integral and the \bar{d}/\bar{u} asymmetry is clearly seen in the parton model, namely,

$$\int_0^1 [F_2^p(x, Q^2) - F_2^n(x, Q^2)]/x dx = \frac{1}{3} + \frac{2}{3} \int_0^1 [\bar{u}(x, Q^2) - \bar{d}(x, Q^2)] dx. \quad (4)$$

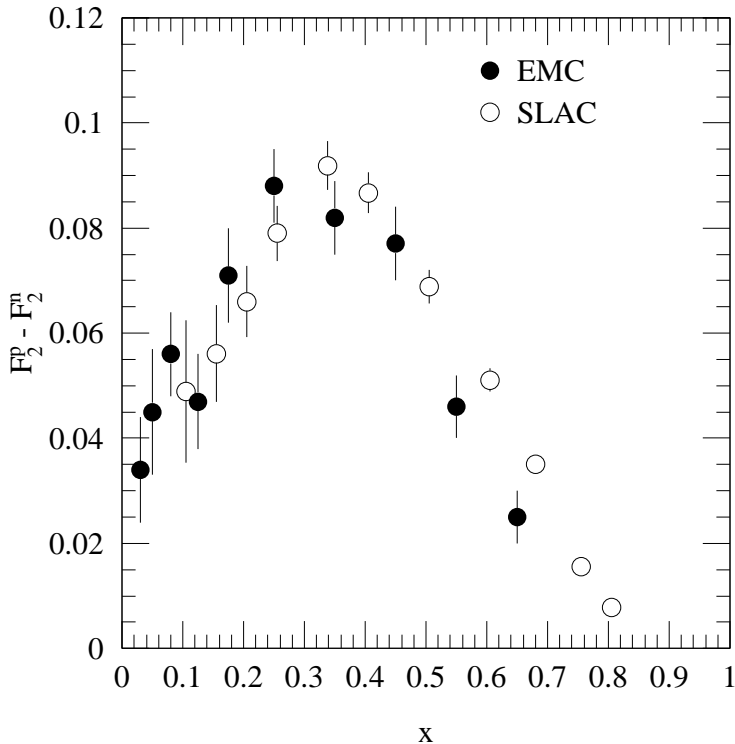


Figure 1: EMC [28] and SLAC [30] measurements of $F_2^p - F_2^n$.

Equation 4 clearly shows that the early SLAC data on GSR implied $\bar{d} > \bar{u}$, at least for certain region of x . Field and Feynman further suggested that Pauli blocking from the valence quarks would inhibit the $\bar{u}u$ sea more than the $\bar{d}d$ sea, hence creating an asymmetric nucleon sea.

The SLAC DIS experiments were followed by several muon-induced DIS experiments at Fermilab and at CERN. Using high energy muon beams, these experiments reached much larger values of Q^2 and they clearly observed [25, 26, 27] the scaling-violation phenomenon in DIS. The Gottfried integral was also evaluated in muon DIS experiments [28, 29]. Figure 1 compares the data from the European Muon Collaboration (EMC) [28] with earlier electron data from SLAC [30]. The coverages in x are similar in these two experiments, even though the Q^2 values covered by the EMC are much larger. Figure 1 shows that $F_2^p - F_2^n$ from EMC tend to shift towards smaller x relative to the SLAC data, in qualitative agreement with the QCD Q^2 -evolution. The Gottfried integral determined from the EMC experiment is $0.235 + 0.110 - 0.099$, consistent with the result from SLAC, but still lower than $1/3$.

Despite the fact that all measurements of the Gottfried integral consistently showed a value lower than $1/3$, the large systematic errors prevented a definitive conclusion. As a result, all parametrizations [31, 32, 33, 34, 35] of the parton distributions based on global fits to existing data before 1990 assumed a symmetric \bar{u}, \bar{d} sea. As discussed next, more compelling evidences for an asymmetric light-quark sea were provided by results from new experiments.

2.3 Drell-Yan Process

The first high-mass dilepton production experiment [36] was carried out at the AGS in 1969, soon after scaling was discovered at SLAC. Drell and Yan [37] interpreted the data within the parton model, in which a quark-antiquark pair annihilate into a virtual photon subsequently decaying into a lepton pair. This simple model was capable of explaining several pertinent features of the data, including the overall

magnitude of the cross sections, the scaling behavior of the cross sections, and the polarization of the virtual photons. The high-mass continuum lepton-pair production is therefore called the Drell-Yan (DY) process.

Since the underlying mechanism for the DY process involves the annihilation of a quark with an antiquark, it is not surprising that this process can be used to probe the antiquark contents of the beam or target hadrons. In the parton model, the DY cross section is given by

$$\frac{d^2\sigma}{dM^2 dx_F} = \frac{4\pi\alpha^2}{9M^2 s} \frac{1}{(x_1 + x_2)} \sum_a e_a^2 [q_a(x_1)\bar{q}_a(x_2) + \bar{q}_a(x_1)q_a(x_2)]. \quad (5)$$

Here $q_a(x)$ and $\bar{q}_a(x)$ are the quark and antiquark parton distributions of the two colliding hadrons evaluated at the momentum fraction x . The sum is over quark flavors. In addition, one has the kinematic relations,

$$\begin{aligned} \tau &\equiv x_1 x_2 = M^2/s, \\ x_F &= x_1 - x_2, \end{aligned} \quad (6)$$

where M is the invariant mass of the lepton pair and s is the square of the center-of-mass energy. The cross section is proportional to α^2 , indicating its electromagnetic character.

Equation 5 shows that the antiquark distribution enters as a multiplicative term in the DY cross section rather than an additive term in the DIS cross section. Hence, the antiquark distributions can be sensitively determined in the DY experiments. The dimuon data from the FNAL E288, in which the Υ resonances were discovered [38], were analysed [39] to extract the sea quark distribution in the nucleon. By assuming a flavor-symmetric nucleon sea, namely, $\bar{u}(x) = \bar{d}(x) = \bar{s}(x) = Sea(x)$, the dimuon mass distribution obtained in 400 GeV proton-nucleus interaction was described by $xSea(x) = 0.6(1-x)^{10}$. In a later analysis [40] taking into account additional data at 200 and 300 GeV, the E288 collaboration found that a much better fit could be obtained with an asymmetric sea, namely,

$$\bar{u}(x) = (1-x)^{3.48}\bar{d}(x), \quad \bar{s}(x) = (\bar{u}(x) + \bar{d}(x))/4. \quad (7)$$

The need for an asymmetric \bar{u} and \bar{d} was also revealed in the E288 $d\sigma/dy$ DY data [40] at $y = 0$, where y is the center-of-mass rapidity. For $p + A$ collision, the slope of $d\sigma/dy$ at $y = 0$ is expected to be positive due to the excess of u over d valence quarks in the proton. The E288 data showed that the slopes are indeed positive, but larger than expected from a flavor symmetric sea. A surplus of \bar{d} over \bar{u} in the proton sea would lead to more positive slope in agreement with the data [40].

The FNAL E439 collaboration [41] studied high mass dimuons produced in $p + W$ interaction at 400 GeV. Their spectrometer covered a considerably larger range in x_F than E288. They again found that an asymmetric sea, $\bar{u}(x) = (1-x)^{2.5}\bar{d}(x)$, could well describe their data.

With all the tantalizing evidence for an asymmetric sea from DIS and DY experiments, it is curious that all global analyses [31, 32, 33, 34, 35] of parton distributions in the 1980's still assumed a symmetric light-quark sea. This probably reflected the reluctance to adopt an unconventional description of the nucleon sea without compelling and unambiguous experimental evidence. As discussed in the next Section, such evidence became available in the 1990's.

3 Recent Experimental Developments

3.1 NMC Measurements of the Gottfried Integral

After the discovery of the so-called ‘EMC effect’ [42] which showed that the parton distributions in heavy nuclei are different from that in the deuteron, the EMC detector system was modified by the

New Muon Collaboration (NMC) at CERN to study in detail the EMC effect. Special emphases were placed on the capability to reach the low- x region where the ‘shadowing effect’ [43] is important, and to measure cross section ratios accurately [44]. By implementing a ‘small angle’ trigger which extended the scattering angle coverage down to 5 mrad, the lowest value of x reached by NMC was ~ 0.001 . The NMC also placed two targets in the muon beam, allowing DIS data from two different targets to be recorded simultaneously, thus greatly reducing the beam flux normalization uncertainty. To account for the different geometric acceptances for events originating from the two targets, half of the data were taken using a target configuration where the locations of the two targets were interchanged.

The upgraded NMC detectors allowed a definitive study [45] of the shadowing effect at low x . Moreover, they enabled a much more accurate determination of the Gottfried integral. Figure 2 shows the $F_2^p - F_2^n$ reported by the NMC in 1991 [46], in which the smallest x reached (0.004) was significantly lower than in previous experiments. Taking advantage of their accurate measurements of the F_2^n/F_2^p ratios, NMC used the following expression to evaluate $F_2^p - F_2^n$, namely,

$$F_2^p - F_2^n = F_2^d (1 - F_2^n/F_2^p)/(1 + F_2^n/F_2^p). \quad (8)$$

The ratio $F_2^n/F_2^p \equiv F_2^d/F_2^p - 1$ was determined from NMC’s F_2^d/F_2^p measurement, while F_2^d ($F_2^d = F_2^p + F_2^n$) was taken from a fit to previous DIS experiments at SLAC [47], Fermilab [27], and CERN [48, 49]. The value of the Gottfried integral for the measured region at $Q^2 = 4 \text{ GeV}^2$ is $S_G(0.004 - 0.8) = 0.227 \pm 0.007(\text{stat}) \pm 0.014(\text{syst})$. The contribution to S_G from $x > 0.8$ was estimated to be 0.002 ± 0.001 . Assuming that $F_2^p - F_2^n$ at $x < 0.004$ behaves as ax^b , NMC estimated $S_G(0 - 0.004) = 0.011 \pm 0.003$. Summing the contributions from all regions of x , NMC obtained $S_G = 0.240 \pm 0.016$, which was significantly below $1/3$. This represented the best evidence thus far that the GSR was indeed violated.

In 1994, NMC reevaluated [50] the Gottfried integral using a new F_2^d parametrization from Ref. [51] and newly determined values of F_2^d/F_2^p . The new F_2^d parametrization include data from SLAC [47], BCDMS [48], as well as NMC’s own measurement [51]. The new NMC results for $F_2^p - F_2^n$ are shown in Fig. 2. Note that the 1994 values are slightly larger (smaller) than the 1991 values at small (large) x . The new evaluation gave $S_G(0.004 - 0.8) = 0.221 \pm 0.008(\text{stat}) \pm 0.019(\text{syst})$, and the Gottfried integral became

$$S_G = 0.235 \pm 0.026. \quad (9)$$

This value is consistent with the earlier number. The new systematic error is larger than the old one, reducing somewhat the overall significance of the NMC measurement. Nevertheless, the violation of the GSR is established at a 4σ level.

More recently, NMC published their final analysis of F_2^d/F_2^p [52] and F_2^d [53, 54]. This analysis included the 90 and 280 GeV data taken in 1986 and 1987, as well as the 1989 data at 120, 200 and 280 GeV. The 1989 data were not used in the earlier evaluations [46, 50] of the Gottfried integral. Based on these new data, NMC reported $S_G(0.004 - 0.8) = 0.2281 \pm 0.0065(\text{stat})$ at $Q^2 = 4 \text{ GeV}^2$ [52]. This agrees within statistical errors with previous NMC results [46, 50].

QCD corrections to various parton-model sum rules have been reviewed recently [55]. The α_s and α_s^2 corrections to the Gottfried integral have been calculated [56, 57] and found to be very small (roughly 0.4 % each at $Q^2 = 4 \text{ GeV}^2$). Therefore, QCD corrections can not account for the large violation of GSR found by the NMC. Although perturbative QCD predicts a weak Q^2 dependence for the Gottfried integral, it has been suggested [58, 59] that due to the non-perturbative origin of the \bar{d} , \bar{u} asymmetry the Q^2 dependence of the Gottfried integral will be anomalous between 1 and 5 GeV^2 . This interesting suggestion remains to be tested by DIS experiments.

3.2 E772 Drell-Yan Experiment

The main goal of the Fermilab experiment E772 was to examine the origin of the EMC effect. Among the many theoretical models which explain the EMC effect [60], the pion-excess model [61] predicted a

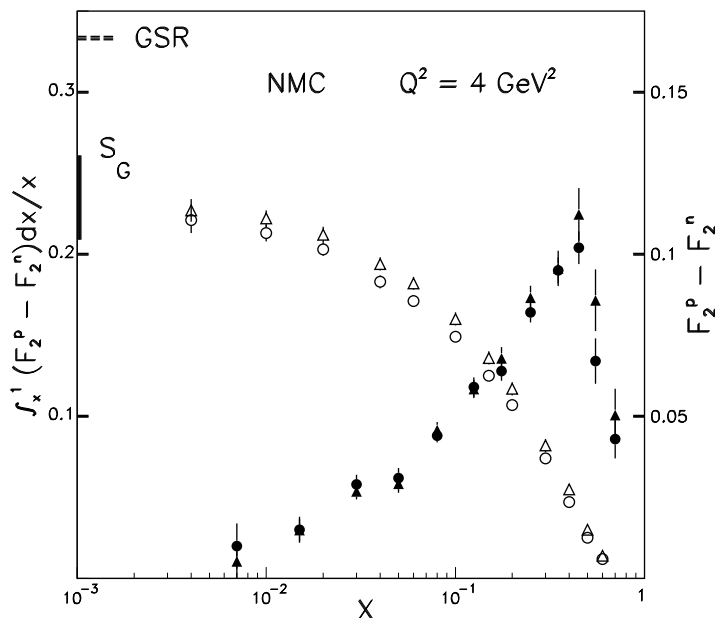


Figure 2: NMC measurements of $F_2^p - F_2^n$ (solid data points) and the Gottfried integral (open data points). The triangular data points correspond to results published in 1991 [46], while the circular data points represent a more recent analysis in 1994 [50]. The extrapolated value of Gottfried integral (S_G) and the expected GSR value are also indicated.

large enhancement of antiquark content due to the presence of additional meson cloud in heavy nuclei. This prediction could be readily tested by measuring the nuclear dependence of proton-induced DY cross sections. Using an 800 GeV proton beam, the DY cross section ratios of a number of nuclear targets (C, Ca, Fe, W) were measured [62] relative to deuterium with high statistics over the region $0.04 < x_2 < 0.35$. The enhancement of antiquark contents predicted by the pion-excess model was not observed, and the E772 results were in good agreement with the prediction of the rescaling model [63].

Information on the \bar{d}/\bar{u} asymmetry has also been extracted from the E772 data [64]. At $x_F > 0.1$, the dominant contribution to the proton-induced DY cross section comes from the annihilation of u quark in the projectile with the \bar{u} quark in the target nucleus. It follows that the DY cross section (per nucleon) ratio of a non-isoscalar target (like $^1H, Fe, W$) over an isoscalar target (like $^2H, ^{12}C, ^{40}Ca$) is given as

$$R_A(x_2) \equiv \sigma_A(x_2)/\sigma_{IS}(x_2) \approx 1 + [(N - Z)/A][(1 - \bar{u}(x_2)/\bar{d}(x_2))/(1 + \bar{u}(x_2)/\bar{d}(x_2))], \quad (10)$$

where x_2 is the Bjorken- x of the target partons, IS stands for isoscalar, and N, Z and A refer to the non-isoscalar target. The $(N - Z)/A$ factor in Eq. 10 shows that the largest sensitivity to the \bar{d}/\bar{u} could be obtained with a measurement of $\sigma(p + p)/\sigma(p + d)$. Nevertheless, for W target $(N - Z)/A = 0.183$ and the E772 σ_W/σ_{IS} data could be used to study the \bar{d}, \bar{u} asymmetry.

Figure 3 shows the E772 DY cross section ratios from the neutron-rich W target over the isoscalar targets, 2H and ^{12}C . Corrections have been applied to the two data points at $x_2 < 0.1$ to account for the nuclear shadowing effects in C and W [64]. The E772 data provided some useful constraints on the \bar{d}/\bar{u} asymmetry. In particular, some early parametrizations [65, 66] of large \bar{d}/\bar{u} asymmetry were ruled out. Despite the relatively large error bars, Figure 3 shows $R > 1.0$ at $x_2 > 0.15$, which is consistent with $\bar{d} > \bar{u}$ in this region.

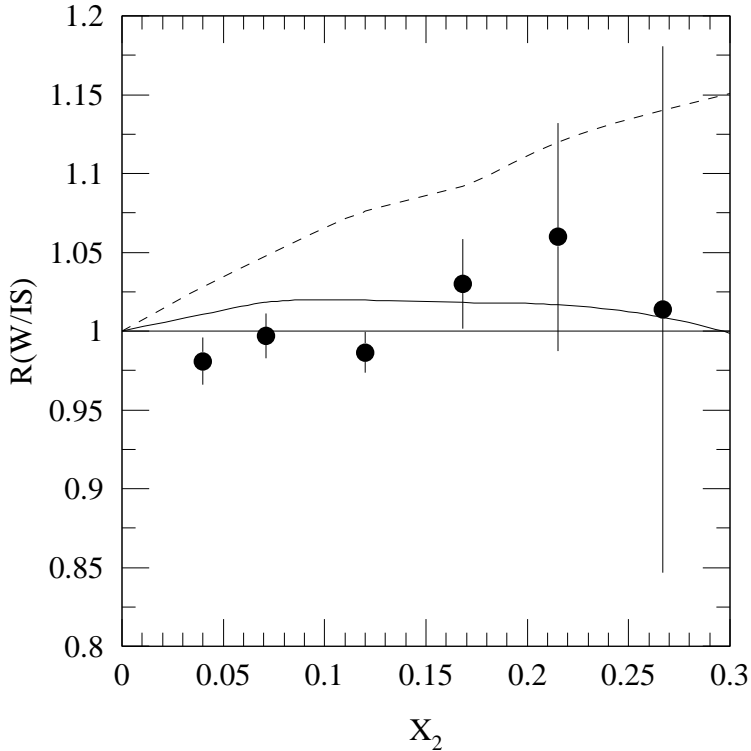


Figure 3: The ratios of W over isoscalar targets DY cross sections from E772 [64]. The dashed curve is a calculation using the \bar{d}/\bar{u} asymmetric parton distributions suggested in Ref. [65]. The solid curve corresponds to a calculation using the MRST distribution functions.

E772 collaboration also presented the DY differential cross sections for $p + d$ at $\langle M_{\mu\mu} \rangle = 8.15$ GeV. As shown in Fig. 4, the DY cross sections near $x_F = 0$ are sensitive to \bar{d}/\bar{u} and the data disfavor a large \bar{d}/\bar{u} asymmetry. Figure 4 also shows that a recent parton distribution function, MRST [67], which has modest \bar{d}/\bar{u} asymmetry, is capable of describing the $p + d$ differential cross sections well (see Section 3.6).

While the E772 data provide some useful constraints on the values of \bar{d}/\bar{u} , it is clear that a measurement of $\sigma_{DY}(p + d)/\sigma_{DY}(p + p)$ is highly desirable. The $(N - Z)/A$ factor is now equal to -1 , indicating a large improvement in the sensitivity to \bar{d}/\bar{u} . Moreover, the uncertainty arising from nuclear effects would be much reduced. It has also been pointed out [68] that \bar{d}/\bar{u} asymmetry in the nucleon could be significantly modified in heavy nuclei through recombination of partons from different nucleons. Clearly, an ideal approach is to first determine \bar{d}/\bar{u} in the nucleon before extracting the \bar{d}/\bar{u} information in heavy nuclei.

3.3 NA51 Drell-Yan Experiment

Following the suggestion of Ellis and Stirling [65], the NA51 collaboration at CERN carried out the first dedicated dimuon production experiment to study the flavor structure of the nucleon sea [69]. Using a 450 GeV proton beam, roughly 2800 and 3000 dimuon events with $M_{\mu\mu} > 4.3$ GeV have been recorded, respectively, for $p + p$ and $p + d$ interaction. The spectrometer setting covers the kinematic region near $y = 0$. At $y = 0$, the asymmetry parameter, A_{DY} , is given as

$$A_{DY} \equiv \frac{\sigma^{pp} - \sigma^{pn}}{\sigma^{pp} + \sigma^{pn}} \approx \frac{(4\lambda_V - 1)(\lambda_s - 1) + (\lambda_V - 1)(4\lambda_s - 1)}{(4\lambda_V + 1)(\lambda_s + 1) + (\lambda_V + 1)(4\lambda_s + 1)}, \quad (11)$$

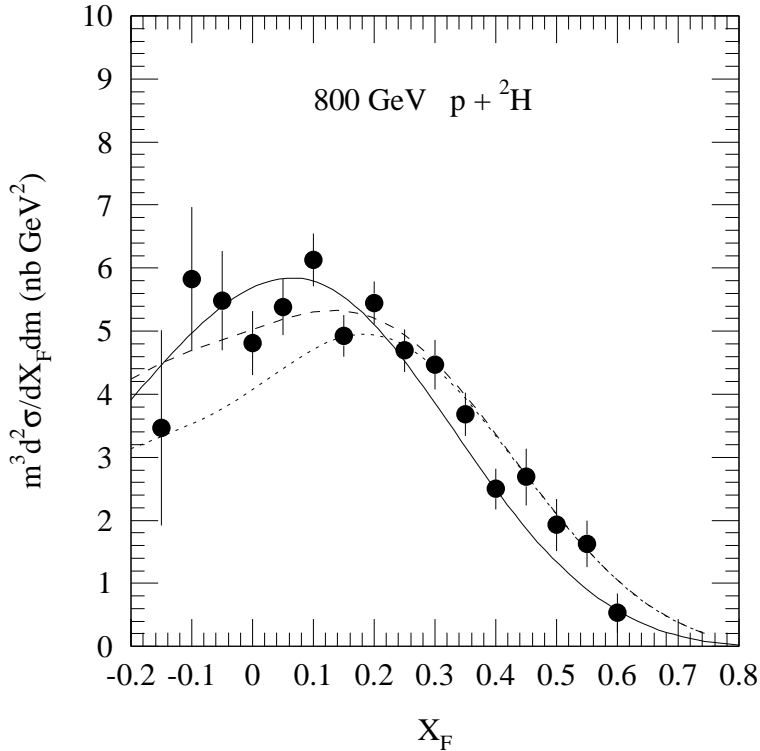


Figure 4: The $p+{}^2H$ DY differential cross sections from E772 [64]. The dotted (dashed) curve is a calculation using the parton distributions from Ref. [65] with (without) \bar{d}/\bar{u} asymmetry. The solid curve uses the MRST distribution functions. These are leading-order calculations normalized to the data.

where $\lambda_V = u_V/d_V$ and $\lambda_s = \bar{u}/\bar{d}$. In deriving Eq. 11, the negligible sea-sea annihilation was ignored and the validity of charge symmetry was assumed. At $x = 0.18$, $\lambda_V \approx 2$ and according to Eq. 11 $A_{DY} = 0.09$ for a symmetric sea, $\lambda_s = 1$. For an asymmetric $\bar{d} > \bar{u}$ sea, A_{DY} would be less than 0.09.

From the DY cross section ratio, σ^{pp}/σ^{pd} , NA51 obtained $A_{DY} = -0.09 \pm 0.02(stat) \pm 0.025(syst)$. This then led to a determination of $\bar{u}/\bar{d} = 0.51 \pm 0.04(stat) \pm (syst)$ at $x = 0.18$ and $\langle M_{\mu\mu} \rangle = 5.22$ GeV. This important result established the asymmetry of the quark sea at a single value of x . What remained to be done was to map out the x -dependence of this asymmetry. This was subsequently carried out by the Fermilab E866/NuSea collaboration, as discussed next.

3.4 E866 Drell-Yan Experiment

At Fermilab, a DY experiment (E866/NuSea) aimed at a higher statistical accuracy with a much wider kinematic coverage than the NA51 experiment was recently completed [70]. This experiment measured the DY muon pairs from 800 GeV proton interacting with liquid deuterium and hydrogen targets. A proton beam with up to 2×10^{12} protons per 20 s spill bombarded one of three identical 50.8-cm long cylindrical target flasks containing either liquid hydrogen, liquid deuterium or vacuum. The targets alternated every few beam spills in order to minimize time-dependent systematic effects. The dimuons accepted by a 3-dipole magnet spectrometer were detected by four tracking stations. An integrated flux of 1.3×10^{17} protons was delivered for this measurement.

Over 330,000 DY events were recorded in E866, using three different spectrometer settings which covered the regions of low, intermediate and high mass muon pairs. The data presented here are from

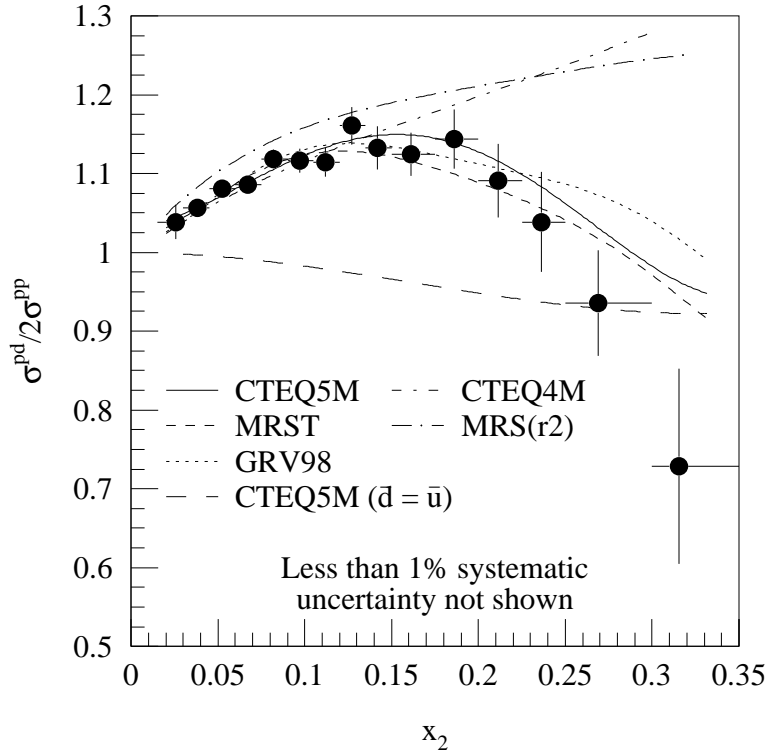


Figure 5: The ratio $\sigma^{pd}/2\sigma^{pp}$ of Drell-Yan cross sections versus x_2 for E866. The curves are next-to-leading order calculations, weighted by acceptance, of the Drell-Yan cross section ratio using various parton distributions. The CTEQ4M and MRS(R2) parton distributions existed prior to the E866 data, while the other distributions came after the E866 results were obtained. In the lower CTEQ5M curve $\bar{d} - \bar{u}$ has been arbitrarily set to 0 as described in the text. The errors are statistical only.

the analysis of the full data set [71]. These data are in good qualitative agreement with the high-mass data published earlier [70]. The DY cross section ratio per nucleon for $p + d$ to that for $p + p$ is shown in Fig. 5 as a function of x_2 . The acceptance of the spectrometer was largest for $x_F = x_1 - x_2 > 0$. In this kinematic regime the DY cross section is dominated by the annihilation of a beam quark with a target antiquark. To a very good approximation the DY cross section ratio at positive x_F is given as

$$\sigma_{DY}(p + d)/2\sigma_{DY}(p + p) \simeq (1 + \bar{d}(x_2)/\bar{u}(x_2))/2. \quad (12)$$

In the case that $\bar{d} = \bar{u}$, the ratio is 1. Figure 5 shows that the DY cross section per nucleon for $p + d$ clearly exceeds $p + p$, and it indicates an excess of \bar{d} with respect to \bar{u} over an appreciable range in x_2 .

Figure 5 also compares the data with next-to-leading order (NLO) calculations of the cross section ratio using the CTEQ4M [72] and the MRS(R2) [73] parton distributions. The data are in reasonable agreement with the predictions for $x_2 < 0.15$. Above $x_2 = 0.15$ the data lie well below the CTEQ4M and the MRS(R2) values. Following the publication of the E866 high-mass data [70], several new parametrizations for parton distributions have been put forward. In Fig. 5 we compare the full E866 data with the calculations using CTEQ5M [74], MRST [67], and GRV98 [75]. Also shown in Fig. 5 is a calculation using a modified CTEQ5M parton distributions. The modified CTEQ5M parton distributions, in which the $\bar{d} + \bar{u}$ parametrization was maintained but \bar{d} was set identical to \bar{u} , were used to illustrate the cross section ratio expected for a symmetric \bar{d}/\bar{u} sea. The E866 data clearly show that $\bar{d} \neq \bar{u}$.

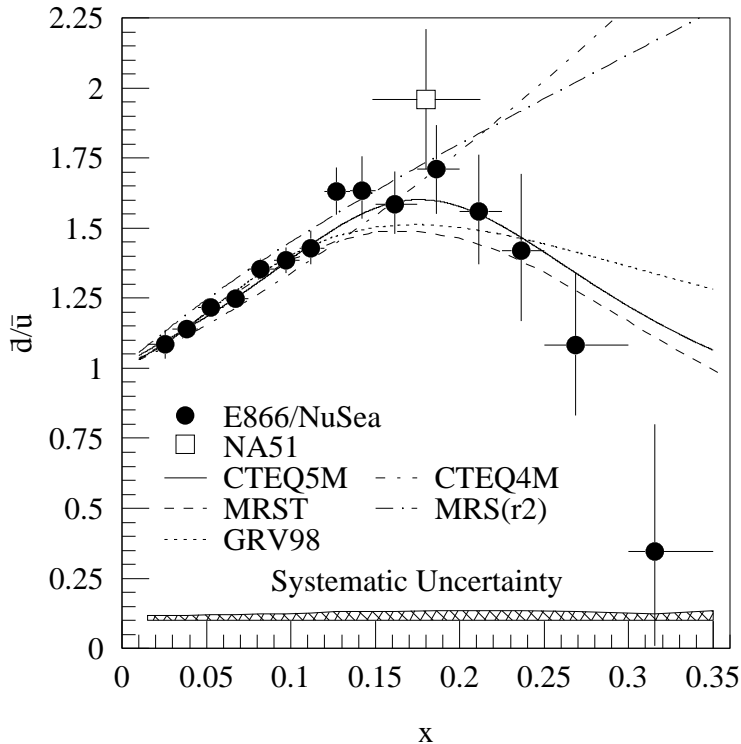


Figure 6: The ratio of \bar{d}/\bar{u} in the proton as a function of x extracted from the Fermilab E866 cross section ratio. The curves are parametrizations of various parton distribution functions. The error bars indicate statistical errors only. Also shown is the result from NA51, plotted as an open box.

Using an iterative procedure described in [70, 71, 76], values for \bar{d}/\bar{u} were extracted by the E866 collaboration at $Q^2 = 54 \text{ GeV}^2$ and shown in Fig. 6. At $x < 0.15$, \bar{d}/\bar{u} increases linearly with x and is in good agreement with the CTEQ4M and MRS(R2) parametrization. However, a distinct feature of the data, not seen in either parametrization of the parton distributions, is the rapid decrease towards unity of the \bar{d}/\bar{u} ratio beyond $x_2 = 0.2$. Figure 6 shows that the most recent parton distribution parametrizations (MRST, CTQ5M, GRV98) adequately describe the E866 data. The result from NA51 is also shown in Figure 6 for comparison.

The \bar{d}/\bar{u} ratios measured in E866, together with the CTEQ5M values for $\bar{d} + \bar{u}$, were used to obtain $\bar{d} - \bar{u}$ over the region $0.02 < x < 0.345$ (Fig. 7). As a flavor non-singlet quantity, $\bar{d}(x) - \bar{u}(x)$ is decoupled from the effects of the gluons and is a direct measure of the contribution from non-perturbative processes, since perturbative processes cannot cause a significant \bar{d} , \bar{u} difference. From the results shown in Fig. 7, one can obtain an independent determination [71] of the integral of $\bar{d}(x) - \bar{u}(x)$ and compare it with the NMC result (Eq. 9). E866 obtains a value $\int_0^1 [\bar{d}(x) - \bar{u}(x)] dx = 0.118 \pm 0.012$, which is 4/5 the value deduced by NMC [50].

The E866 data also allow the first determination [76] of the difference of the momentum fraction carried by \bar{d} and \bar{u} . One obtains $\int_{0.02}^{0.345} x [\bar{d}(x) - \bar{u}(x)] dx = 0.0065 \pm 0.0010$ at $Q^2 = 54 \text{ GeV}^2$. If CTEQ4M is used to estimate the contributions from the unmeasured x regions, one finds that $\int_0^1 x [\bar{d}(x) - \bar{u}(x)] dx = 0.0075 \pm 0.0011$. Unlike the integral of $\bar{d}(x) - \bar{u}(x)$, the momentum integral is Q^2 dependent and decreases as Q^2 increases. The Q^2 dependence of the momentum fraction carried by various partons are shown in Fig. 8. The calculation uses both the MRS(R2) and the new MRST [67]

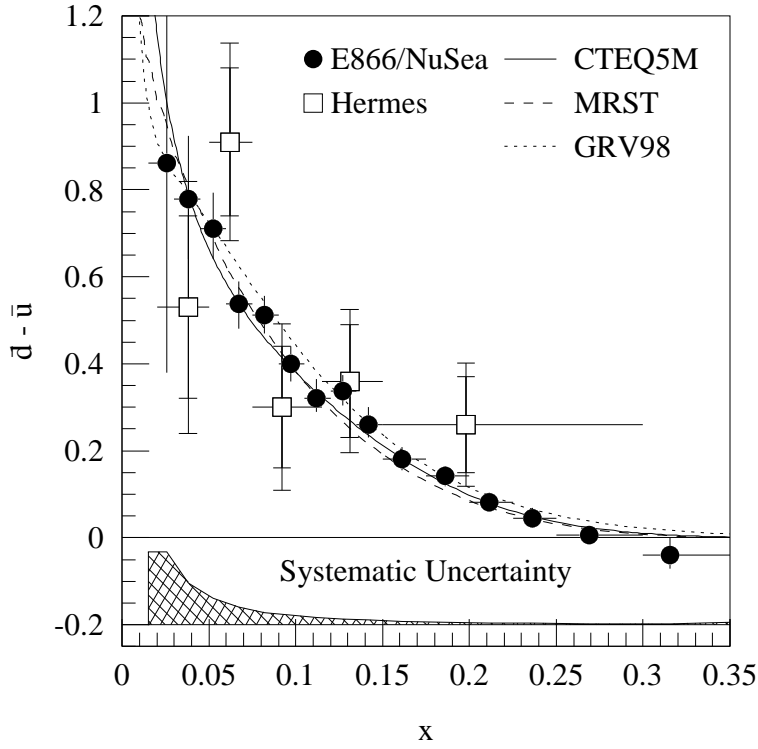


Figure 7: Comparison of the E866 [70] $\bar{d} - \bar{u}$ results at $Q^2 = 54 \text{ GeV}^2$ with the parametrizations of various parton distribution functions. The data from HERMES [82] are also shown.

parton distributions for comparison. Figure 8 shows that the momentum fractions carried by the sea quarks increase with Q^2 . In contrast, the difference of the momentum fraction carried by up and down sea quarks decreases with Q^2 .

3.5 HERMES Semi-Inclusive Experiment

It has been recognized for some time that semi-inclusive DIS could be used to extract the flavor dependence of the valence quark distributions [77]. From quark-parton model, the semi-inclusive cross section, σ_N^h , for producing a hadron on a nucleon is given by

$$\frac{1}{\sigma_N(x)} \frac{d\sigma_N^h(x, z)}{dz} = \frac{\sum_i e_i^2 f_i(x) D_i^h(z)}{\sum_i e_i^2 f_i(x)}, \quad (13)$$

where $D_i^h(z)$ is the fragmentation function signifying the probability for a quark of flavor i fragmenting into a hadron h carrying a fraction z of the initial quark momentum. e_i and f_i are the charge and the distribution function of quark i , and $\sigma_N(x)$ is the inclusive DIS cross section. Assuming charge symmetry for the fragmentation functions and parton distribution functions, one can derive the relationship

$$\frac{d_v(x)}{u_v(x)} = \frac{4R^\pi(x) + 1}{4 + R^\pi(x)}, \quad (14)$$

where

$$R^\pi(x) = (d\sigma_n^{\pi^+}(x, z)/dz - d\sigma_n^{\pi^-}(x, z)/dz) / (d\sigma_p^{\pi^+}(x, z)/dz - d\sigma_p^{\pi^-}(x, z)/dz). \quad (15)$$

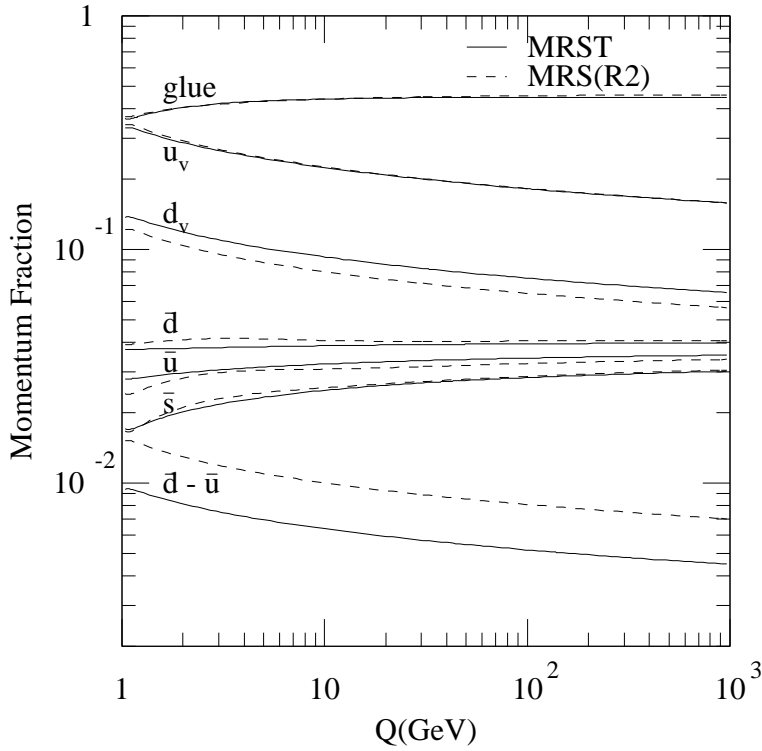


Figure 8: Q -dependence of the proton's momentum carried by various partons calculated using the MRS(R2) and MRST parton distribution functions.

Based on a large number of semi-inclusive charged-hadron events in muon DIS from hydrogen and deuterium targets, EMC extracted [78] the values of $d_v(x)/u_v(x)$ over the range $0.028 < x < 0.66$. The EMC result agrees with neutrino measurements [79, 80], and it demonstrates the usefulness of semi-inclusive measurements for extracting valence quark distributions.

Soon after the report of GSR violation by the NMC, Levelt, Mulders and Schreiber [81] pointed out that semi-inclusive DIS could also be used to study the flavor dependence of sea quarks. In particular,

$$\frac{\bar{d}(x) - \bar{u}(x)}{u(x) - d(x)} = \frac{J(z)[1 - r(x, z)] - [1 + r(x, z)]}{J(z)[1 - r(x, z)] + [1 + r(x, z)]}, \quad (16)$$

where

$$r(x, z) = \frac{d\sigma_p^{\pi^-}(x, z)/dz - d\sigma_n^{\pi^-}(x, z)/dz}{d\sigma_p^{\pi^+}(x, z)/dz - d\sigma_n^{\pi^+}(x, z)/dz}, \quad J(z) = \frac{3}{5} \frac{1 + D_u^{\pi^-}(z)/D_u^{\pi^+}(z)}{1 - D_u^{\pi^-}(z)/D_u^{\pi^+}(z)}. \quad (17)$$

Unlike the situation for $d_v(x)/u_v(x)$ which is completely independent of the fragmentation functions, Equation 16 shows that fragmentation functions are needed to extract the values of $\bar{d}(x) - \bar{u}(x)$.

The HERMES collaboration [82] at DESY recently reported their measurements of charged hadrons produced in the scattering of a 27.5 GeV positron beam on internal hydrogen, deuterium, and ^3He target. The fragmentation functions $D_i^{\pi^\pm}(z)$ were extracted from the ^3He data, while the hydrogen and deuterium data allowed a determination of $r(x, z)$. The values of $(\bar{d} - \bar{u})/(u - d)$ show no z dependence and are positive over the region $0.02 < x < 0.3$, showing clearly an excess of \bar{d} over \bar{u} . Using the GRV94 LO [83] parametrization of $u(x) - d(x)$, the HERMES collaboration obtained $\bar{d}(x) - \bar{u}(x)$ as shown in Fig. 7. The integral of $\bar{d} - \bar{u}$ over the measured x region gives $\int_{0.02}^{0.3} [\bar{d}(x) - \bar{u}(x)] dx =$

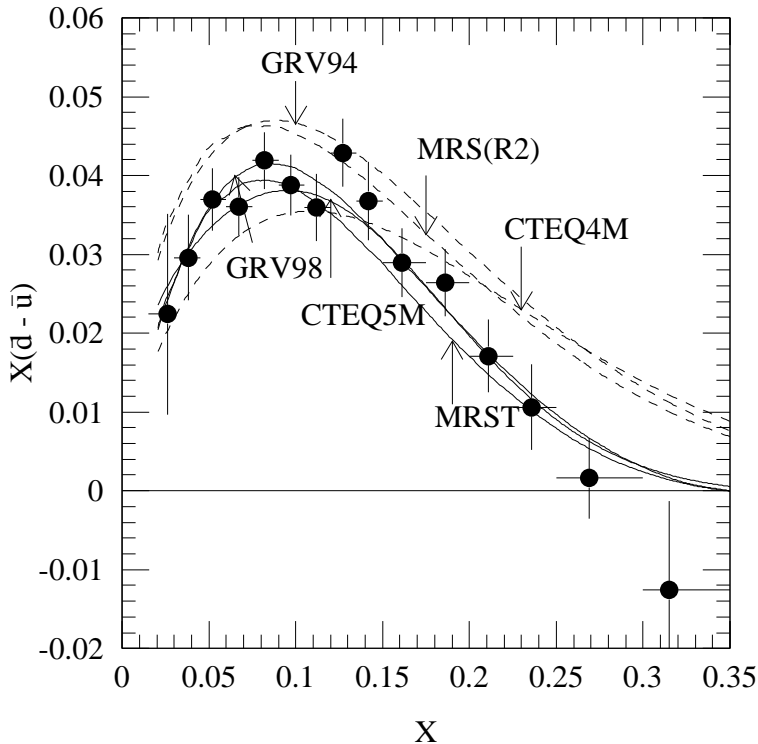


Figure 9: Comparison between the $x(\bar{d} - \bar{u})$ results from E866 with the parametrizations of various parton distribution functions. The dashed (solid) curves correspond to PDFs before (after) the E866 results were obtained.

$0.107 \pm 0.021(stat) \pm 0.017(syst)$. The total integral over all x is extrapolated to be 0.16 ± 0.03 , consistent with the result from NMC. It is gratifying that the results from E866 and HERMES are in rather good agreement, even though these two experiments use very different methods and cover very different Q^2 values ($\langle Q^2 \rangle = 54 \text{ GeV}^2$ in E866 and $\langle Q^2 \rangle = 2.3 \text{ GeV}^2$ in HERMES).

It should be mentioned that semi-inclusive DIS could be extended [84, 85] to situations involving polarized lepton beam and polarized targets in order to study the flavor dependence of the spin-dependent structure functions. Both the Spin Muon Collaboration (SMC) [86] and the HERMES Collaboration [87] have reported the polarized valence quark distributions, $\Delta u_v(x)$ and $\Delta d_v(x)$, and the non-strange sea-quark polarization, $\Delta \bar{q}(x)$.

3.6 Impact on the Parton Distribution Functions

After the evidence for a flavor asymmetric sea was reported by the NMC and NA51, several groups [72, 73, 83] performing global analysis of parton distribution functions all required \bar{d} to be different from \bar{u} . The NMC result constrained the integral of $\bar{d} - \bar{u}$ to be 0.149 ± 0.039 , while the NA51 result requires \bar{d}/\bar{u} to be 1.96 ± 0.13 at $x = 0.18$. Clearly, the x dependences of $\bar{d} - \bar{u}$ and \bar{d}/\bar{u} were undetermined. Figures 6 and 9 compare the E866 measurements of \bar{d}/\bar{u} and $x(\bar{d} - \bar{u})$ with the parametrizations of the MRS(R2) [73] and CTEQ4M [72], two of the most frequently used PDF's prior to E866's measurement.

Recently, several PDF groups published new parametrizations taking into account of new experimental information including the E866 data. The parametrization of the x dependence of $\bar{d} - \bar{u}$ is now strongly constrained by the E866 and HERMES data. In particular, $\bar{d}(x) - \bar{u}(x)$ or $\bar{d}(x)/\bar{u}(x)$ are parametrized as follows;

MRST [67]:

$$\bar{d}(x) - \bar{u}(x) = 1.29x^{0.183}(1-x)^{9.808}(1 + 9.987x - 33.34x^2), \quad Q_0^2 = 1 \text{ GeV}^2,$$

GRV98 [75]:

$$\bar{d}(x) - \bar{u}(x) = 0.20x^{-0.57}(1-x)^{12.4}(1 - 13.3x^{0.5} + 60.0x), \quad Q_0^2 = 0.4 \text{ GeV}^2,$$

CTEQ5M [74, 88]:

$$\bar{d}(x)/\bar{u}(x) = 1 - 1.095x + 3.159x^{0.5}/[1 + (x - 0.188)^2/0.01346], \quad Q_0^2 = 1 \text{ GeV}^2. \quad (18)$$

As shown in Fig. 6, these new parametrizations give significantly different shape for \bar{d}/\bar{u} at $x > 0.15$ compared to previous parametrizations. Table 1 also lists the values of $\bar{d} - \bar{u}$ integral from various various experiments and from recent PDF's.

Table 1: Values of the integral $\int_0^1(\bar{d}(x) - \bar{u}(x))dx$ from various experiments and parton distribution functions.

Experiment/PDF	Integral
NMC	0.148 ± 0.039
E866	0.118 ± 0.012
HERMES	0.16 ± 0.03
CTEQ4M	0.108
MRS(R2)	0.162
GRV94	0.163
CTEQ5M	0.124
MRST	0.102
GRV98	0.126

It is interesting to note that the E866 data also affect the parametrization of the valence-quark distributions. Figure 10 shows the NMC data for $F_2^p - F_2^n$ at $Q^2 = 4 \text{ GeV}^2$, together with the fits of MRS(R2) and MRST. It is instructive to decompose $F_2^p(x) - F_2^n(x)$ into contributions from valence and sea quarks:

$$F_2^p(x) - F_2^n(x) = \frac{1}{3}x[u_v(x) - d_v(x)] + \frac{2}{3}x[\bar{u}(x) - \bar{d}(x)]. \quad (19)$$

As shown in Fig. 10, the E866 data provide a direct determination of the sea-quark contribution to $F_2^p - F_2^n$. In order to preserve the fit to $F_2^p - F_2^n$, the MRST's parametrization for the valence-quark distributions, $u_v - d_v$, is significantly lowered in the region $x > 0.01$. Indeed, one of the major new features of MRST is that d_v is now significantly higher than before at $x > 0.01$. Although the authors of MRST attribute this to the new W -asymmetry data from CDF [89] and the new NMC results on F_2^d/F_2^p [52], it appears that the new information on $\bar{d}(x) - \bar{u}(x)$ has a direct impact on the valence-quark distributions too.

Another implication of the E866 data is on the behavior of $F_2^p - F_2^n$ at small x . In order to satisfy the constraint $\int_0^1[u_v(x) - d_v(x)]dx = 1$, the MRST values of $u_v(x) - d_v(x)$ at $x < 0.01$ are now much larger than in MRS(R2), since $u_v(x) - d_v(x)$ at $x > 0.01$ are smaller than before. As a consequence, $F_2^p - F_2^n$ is increased at small x and MRST predicts a large contribution to the Gottfried integral from the small- x ($x < 0.004$) region, as shown in Fig. 11. If the MRST parametrization for $F_2^p - F_2^n$ at $x < 0.004$ were used, NMC would have deduced a value of 0.252 for the Gottfried integral, which would imply a value of 0.122 for the $\bar{d} - \bar{u}$ integral. This would bring excellent agreement between the E866 and the NMC results on the $\bar{d} - \bar{u}$ integral.

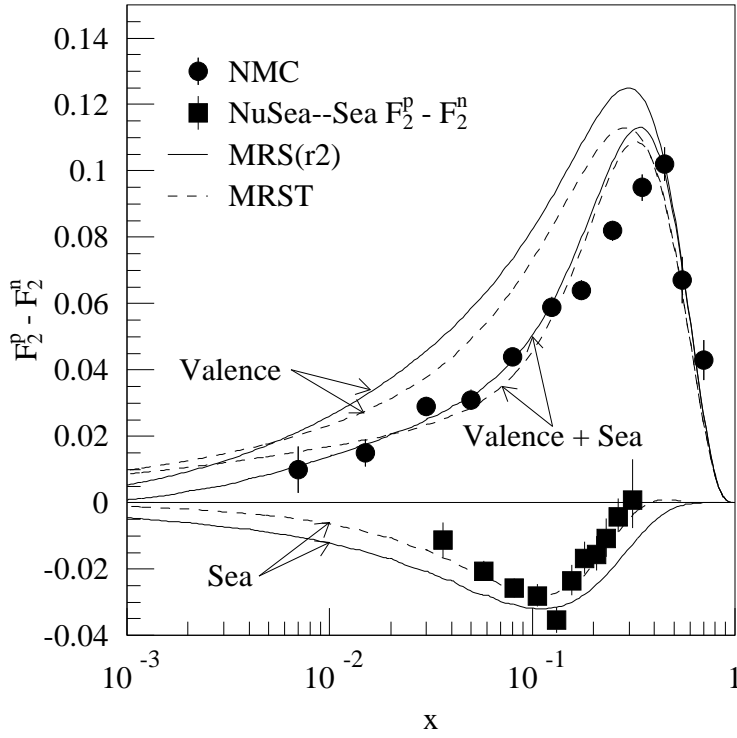


Figure 10: $F_2^p - F_2^n$ as measured by NMC at $Q^2 = 4 \text{ GeV}^2$ compared with predictions based on the MRS(R2) and MRST parametrizations. Also shown are the E866/NuSea results, rescaled to $Q^2 = 4 \text{ GeV}^2$, for the sea-quark contribution to $F_2^p - F_2^n$. For each prediction, the top (bottom) curve is the valence (sea) contribution and the middle curve is the sum of the two.

3.7 Comparison Between Various Measurements

Are the various measurements of sea quark flavor asymmetry consistent among them? In particular, is the E866 result consistent with the earlier E772 and the NA51 DY experiments, and with the HERMES and NMC DIS measurements? To address this question, we first compare E866 with E772, both of which are DY experiments using 800 GeV proton beam with essentially the same spectrometer. Figs. 3 and 4 show that the MRST parton distributions, which determined $\bar{d} - \bar{u}$ based on the E866 data, can also describe the E772 data very well, and we conclude that the E866 and E772 results are consistent.

Although both NA51 and E866 measured $\sigma(p+d)/2\sigma(p+p)$ to extract the values of \bar{d}/\bar{u} , some notable differences exist. As mentioned earlier, NA51 measured the ratio at a single value of x_2 ($x_2 = 0.18$) near $x_F \approx 0$ using a 450 GeV proton beam, while E866 used an 800 GeV proton beam to cover a broader range of x_2 at $x_F > 0$. It is instructive to compare the NA51 result at $x_2 = 0.18$ with the E866 data at $x_2 = 0.182$. Table 2 lists the kinematic variables and physics quantities derived from these two data points. It is interesting to note that the values of $\sigma(p+d)/2\sigma(p+p)$ at $x_2 = 0.18$ are actually very similar for NA51 and E866, even though the derived values for \bar{d}/\bar{u} differ significantly. This reflects the difference in x_F for both experiments, making the values of \bar{d}/\bar{u} extracted from $\sigma(p+d)/2\sigma(p+p)$ different. The other difference is Q^2 , being a factor of 3.6 higher for E866. Using MRST and CTEQ5M to estimate the Q^2 dependence of \bar{d}/\bar{u} , we find that the NA51 value of \bar{d}/\bar{u} is reduced by $\approx 3\%$ going from $Q^2 = 27.2 \text{ GeV}^2$ to $Q^2 = 98.0 \text{ GeV}^2$. This brings slightly better agreement between NA51 and E866.

The methods used by HERMES and E866 to determine $\bar{d} - \bar{u}$ are different, and it is reassuring that

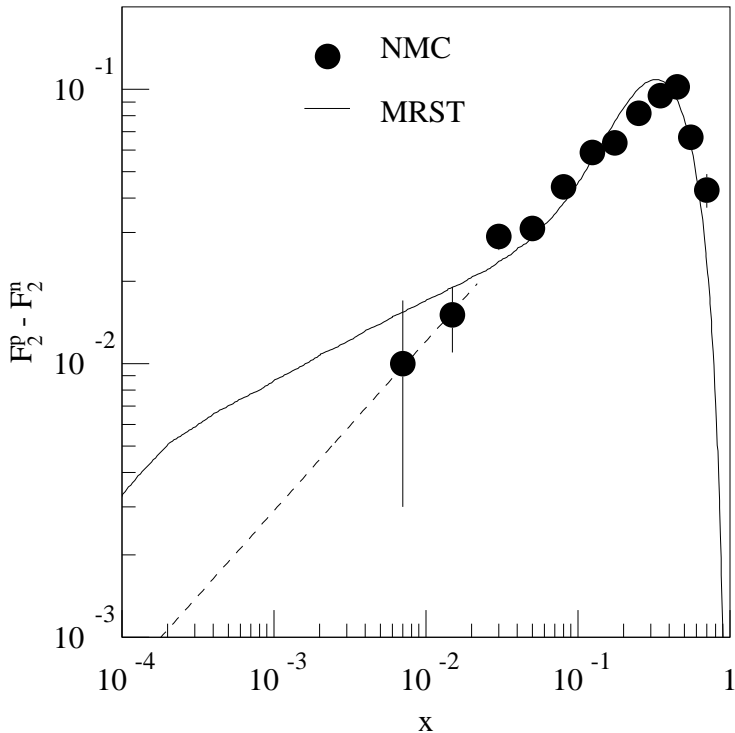


Figure 11: $F_2^p - F_2^n$ as measured by NMC at $Q^2 = 4 \text{ GeV}^2$ compared with parametrization of MRST. The dashed curve corresponds to $0.21x^{0.62}$, a parametrization assumed by the NMC for the unmeasured small- x region when the Gottfried integral was evaluated.

Table 2: Comparison between the 450 GeV NA51 result and the 800 GeV E866 data point [70] near $x_2 = 0.18$.

	$\langle x_2 \rangle$	$\langle x_F \rangle$	$\langle M_{\mu\mu} \rangle (\text{GeV})$	$\sigma^{pd}/2\sigma^{pp}$	\bar{d}/\bar{u}
NA51	0.18	0.0	5.2	1.099 ± 0.039	1.96 ± 0.246
E866	0.182	0.192	9.9	1.091 ± 0.044	1.41 ± 0.146

the results came out alike, as shown in Fig. 7. The $\bar{d} - \bar{u}$ values from HERMES are in general somewhat larger than those of E866. At a relatively low mean Q^2 of 2.3 GeV^2 , the HERMES experiment could be subject to high-twist effects [90]. Additional data from HERMES are expected to improve the statistical accuracy.

The comparison between E866 and NMC in terms of the integral of $\bar{d} - \bar{u}$ has been discussed earlier. A possible origin for the apparent differences of the integral was also discussed in Section 3.6.

4 Origins of the \bar{d}/\bar{u} Asymmetry

The earliest DIS experiments indicated that the Gottfried integral was less than $1/3$, leading to speculation regarding the origin of this reduction. Field and Feynman suggested [24] that it could be due to Pauli blocking in so far as $u\bar{u}$ pairs would be suppressed relative to $d\bar{d}$ pairs because of the presence of two u -quarks in proton as compared to a single d -quark. Ross and Sachrajda [56] questioned that this effect would be appreciable because of the large phase-space available to the created $q\bar{q}$ pairs. They

also showed that perturbative QCD would not produce a \bar{d}, \bar{u} asymmetry. Steffens and Thomas [91] recently looked into this issue, explicitly examining the consequences of Pauli blocking. They similarly concluded that the blocking effects were small, particularly when the antiquark is in a virtual meson.

The small d, u mass difference (actually, $m_d > m_u$) of 2 to 4 MeV compared to the nucleon confinement scale of 200 MeV does not permit any appreciable difference in their relative production by gluons. At any rate, one observes a surplus of \bar{d} which is the heavier of the two species. As pointed out above, blocking effects arising from the Pauli exclusion principle should also have little effect. Thus another, presumably non-perturbative, mechanism must be found to account for the large measured \bar{d}, \bar{u} asymmetry.

As many of the non-perturbative approaches to explain the asymmetry involve the use of isovector mesons (particularly pions), we present some of the motivation for believing that pion field is intrinsic to the nucleon's makeup.

4.1 *The Nucleon's Mesonic Field in Strong and Electroweak Process*

The requirement of the pion as intrinsic to the nucleon has been evident to most who have addressed the nucleon's interactions. To address the nucleon's partonic structure as totally independent of its interactions seems naive indeed. However, the success of the constituent quark model in simply and directly explicating nucleon properties has focused attention on the quark structure of the nucleon to the point that the role of pions was obscured. The magnetic moments of baryons are well characterized by constituent quarks, and pions are now known to have little effect on the result [92]. In its most extreme form there was a hope to start with three constituent quarks at some low Q^2 scale and simply employ QCD evolution to generate nucleon's observed partonic distributions. We now know this is most unlikely if not impossible, as non-singlet quantities such as g_A , the \bar{u}, \bar{d} asymmetry, are of a non-perturbative origin and must be inserted ab initio if the nucleon's parton distributions are to be properly characterized. In the following we list properties of the nucleon that require it to possess a meson cloud.

- The nucleon's strong interactions, particularly the long-range part of the nucleon-nucleon interaction have been characterized via meson exchange. The development of a low energy nucleon-nucleon potential has gone on for many years [93, 94] with the long-range part in particular requiring a dominant role for pion exchange. Attempts to generate this interaction from QCD-inspired models [95, 96] have not met with quantitative success [97] so need for meson-exchange to account for the medium- and long-range parts of the nucleon-nucleon interaction appears beyond doubt.
- The requirement that the nucleon axial current be partially conserved (PCAC) requires the pion to be an active participant in the nucleon. As the pion is the axial charge, it has a dominant status in PCAC. Figure 12 is a diagram of the pion's role in nucleon beta decay. Employing PCAC, the Goldberger-Treiman [98] relation can easily be derived,

$$g_A = \frac{F_\pi g_c}{M_p}. \quad (20)$$

In the above expression F_π is the pion decay constant (92.42 ± 0.26 MeV), g_c is the charged pion (πnp) coupling constant ($4\pi(14.17 \pm 0.2)^{1/2}$) [99] and M_p the proton mass. This yields a value for g_A that is (3.8 ± 2.5) % too high, not inconsistent with the variance expected due to the breaking of chiral symmetry ($m_u, m_d, m_\pi \neq 0$). Furthermore, the value of the induced pseudoscalar form factor, $g_p(Q^2)$, is also directly dependent on the pionic field of the nucleon. PCAC yields a result [100]

$$g_p(Q_0^2 = -0.88m_\mu^2) = 8.44 \pm 0.23, \quad (21)$$

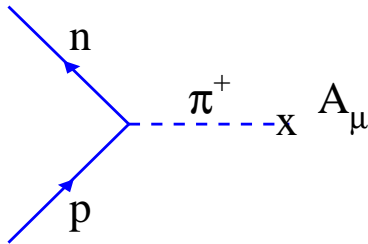


Figure 12: Diagram showing pion's role in nucleon beta decay.

consistent, albeit with large errors, with the measured value,

$$g_p(Q_0^2) = 8.7 \pm 2.9. \quad (22)$$

There are of course many other examples where mesons, especially the pion are employed to account for the nucleon's properties. Indeed, QCD based chiral models have treated the pion as a basic degree of freedom from the earliest times [101]. However, the consequences of their effects were not incorporated into parton distributions until the early 90's [102, 103].

As is well known, the information on the nucleon's structure from parity-conserving elastic electron scattering is contained in four form factors. They are the Dirac ($F_1(Q^2)$) and Pauli ($F_2(Q^2)$) form factors for the neutron and proton. Linear combinations of these form factors are often employed, for example an isoscalar ($F^p + F^n$) and an isovector ($F^p - F^n$) combination as well as the Sachs [104] electric and magnetic form factors:

$$G_E(Q^2) = F_1(Q^2) - \frac{Q^2}{4M^2} F_2(Q^2); \quad G_M(Q^2) = F_1(Q^2) + F_2(Q^2). \quad (23)$$

The normalization of the form factors are $F_1^p(0) = 1$, $F_1^n(0) = 0$, $F_2^p(0) = 1.793$, and $F_2^n(0) = -1.913$. The Sachs form factors are just the Fourier transforms of the charge and magnetization distributions in the Breit frame.

The large body of electron scattering data spanning $0 < Q^2 < 30 \text{ GeV}^2$ can be analyzed in a largely model independent fashion using dispersion relations. They fit the data rather well but are not very revealing of the underlying structure of the nucleon. The electric form factor of the neutron on the other hand could be most revealing regarding the presence of a $p\pi^-$ component in the neutron wave function. There are two difficulties to be faced. First, the presence of the Foldy term in $G_E^n(Q^2)$ tends to obscure and complicate the interpretation of the neutron charge distribution [105]. Secondly, there are QCD hyperfine interactions [105, 106, 107] that produce a negative neutron charge radius similar to the $p\pi^-$ component. Thus it will take extensive additional theoretical and experimental work to clarify this important issue in electron-nucleon scattering. However, some promising steps are being taken [108].

An area where appreciable recent progress has been made is in the analysis of the nucleon's electromagnetic form factors in terms of relativistic baryon chiral perturbation theory [109]. This approach is the effective theory of QCD at low energy, which limits its range of applicability to $\sim Q^2 < 0.5 \text{ GeV}^2$. The vector mesons are brought in without the introduction of additional parameters by using the results of theoretical dispersion analysis of the form factors. The neutron charge form factor is little changed by the inclusion of vector mesons, while they have a beneficial effect on the three other nucleon form factors. Figure 13 shows the level of agreement obtained in $G_E^n(Q^2)$ applying relativistic baryon chiral

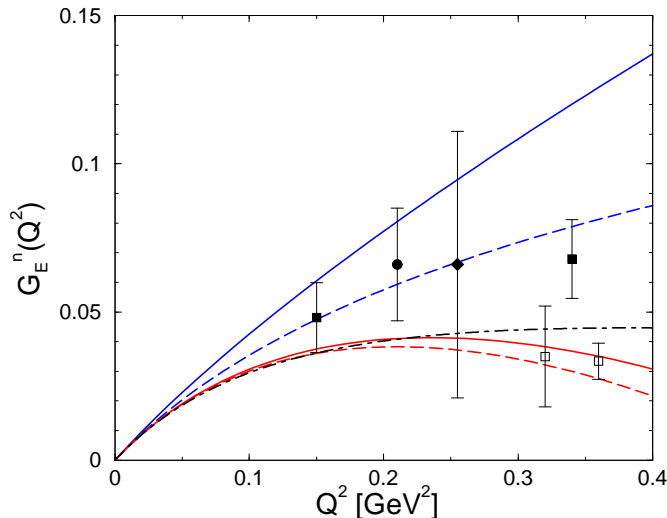


Figure 13: Comparison between data and calculations [109] using relativistic baryon chiral perturbation theory for $G_E^n(Q^2)$. The dashed curves are the results of calculation without vector mesons, the upper dashed curve being to 3rd order while the lower is to 4th order. The solid curves are the results including vector mesons where the upper curve is to 3rd order while the lower is to 4th order. The dot-dashed curve is the result of the dispersion theoretical analysis.

perturbation theory as shown in Ref. [109]. While the fits are impressive it still remains illusive as to what is added to our picture of the nucleon. The pion field determines most of the properties of the form factors. For example, the leading terms for the radii of the isovector charge and magnetic form factors [108] are

$$\langle r_1^v \rangle^2 = \frac{10g_A^2 + 2}{(4\pi F_\pi)^2} \ln \frac{M_\pi}{m_N}; \quad \langle r_2^v \rangle^2 = \frac{g_A^2 m_N}{8\pi F_\pi^2 \kappa_v M_\pi}, \quad (24)$$

where κ_v is the nucleon anomalous isovector magnetic moment (3.706). Note that in the chiral limit ($M_\pi \rightarrow 0$), both radii become infinite, a not surprising result for massless pions. Our main purpose is to show that the pion mass is a critical parameter in the nucleon form factors in this chiral model derived from QCD. The important role of pions in the structure of the nucleon appears to us to be beyond question and the nucleon's parton distributions should reflect this.

4.2 Meson-Cloud Models

As the \bar{u}, \bar{d} asymmetry cannot be generated via perturbative process, several non-perturbative models have been proposed that yield an asymmetry. The most straightforward of these models are those that attribute the asymmetry to the existence of a “pion cloud” in the proton. The relevance of pion cloud for sea-quark distributions appears to have first been made by Thomas in a publication [110] treating SU(3) symmetry breaking in the nucleon sea. Sullivan [111] had earlier shown that virtual meson-baryon states directly contribute to the nucleon's structure function. A large number of authors have contributed to calculating the asymmetry from this perspective, so recent reviews [112, 113] should be consulted for a complete list of contributions.

In the meson-cloud model, the virtual pion is emitted by the proton and the intermediate state is pion + baryon. More specifically, the proton is taken to a linear combination of a “bare” proton plus

pion-nucleon and pion-delta states, as below,

$$|p\rangle \rightarrow \sqrt{1-a-b}|p_0\rangle + \sqrt{a}(-\sqrt{\frac{1}{3}}|p_0\pi^0\rangle + \sqrt{\frac{2}{3}}|n_0\pi^+\rangle) + \sqrt{b}(\sqrt{\frac{1}{2}}|\Delta_0^+\pi^-\rangle - \sqrt{\frac{1}{3}}|\Delta_0^+\pi^0\rangle + \sqrt{\frac{1}{6}}|\Delta_0^0\pi^+\rangle). \quad (25)$$

The subscript zeros on the virtual baryon states indicate that they are assumed to have symmetric seas, so the asymmetry in the antiquarks must be generated from the pion valence distribution. The coefficients a and b are the fractions of the πN and $\pi\Delta$ configurations, respectively, in the proton. These fractions can be calculated using the πNN and $\pi N\Delta$ couplings, and form factors as taken from experiment. The asymmetry in the proton sea arises because of the dominance of π^+ among the virtual configurations. These calculations, to be discussed in detail below, reproduce many aspects of the data but suffer two problems. First, there is a strong dependence on the value used to cut off the integral over the form factor, and secondly, any such calculation of $\bar{d}(x)/\bar{u}(x)$ is unreliable because the magnitude of the symmetric sea is unknown. Before launching into a more detailed presentation of these calculation, a few general observations can be made. It is instructive to examine some general properties of the πN , $\pi\Delta$ ansatz. A useful expression to consider is

$$\frac{\bar{d}_p(x)}{\bar{u}_p(x)} = \frac{\frac{5}{6}af_\pi^N(x) + \frac{1}{3}bf_\pi^\Delta(x) + \frac{1}{2}S(x)}{\frac{1}{6}af_\pi^N(x) + \frac{2}{3}bf_\pi^\Delta(x) + \frac{1}{2}S(x)}. \quad (26)$$

$S(x)$ is the amount of symmetric sea and $f_\pi^N(x)$ ($f_\pi^\Delta(x)$) are functions that characterize the distributions in x associated with the πN ($\pi\Delta$) configurations. From this expression it is clear that the magnitude of the symmetric sea must be known if the ratio is to be predicted. The maximum value that the ratio can assume is 5, if there were no symmetric sea and only πN configurations contribute. The minimum value of the ratio is 1/2 which occurs in the absence of a symmetric sea and only $\pi\Delta$ configurations contributing. The ratio takes on a value 1 with a pure symmetric sea, or a symmetric sea with $a = b/2$ and $f_\pi^N = f_\pi^\Delta$. Pion models are much more effective in dealing with the integral isolating the contribution from asymmetric sea (AS)

$$I_{AS} \equiv \int_0^1 [\bar{d}_p(x) - \bar{u}_p(x)] dx = \frac{1}{3}(2a - b), \quad (27)$$

as there is no contribution from the symmetric sea in this case.

Many attempts [114, 115, 116, 117, 118, 119, 120] have been made to calculate the flavor asymmetry due to isovector mesons. Most start with the following convolution expressions:

$$x\bar{q}_p(x, Q^2) = \sum_{MB} a_{MB}^p \int_x^1 dy f_{MB}(y) \frac{x}{y} \bar{q}_M\left(\frac{x}{y}, Q^2\right), \quad (28)$$

where

$$f_{MB}(y) = \frac{g_{MpB}^2}{16\pi^2} y \int_{-\infty}^{t_{min}} dt \frac{F(t, m_p, m_B)}{(t - m_M^2)^2} F_{MpB}^2(t, \Lambda), \quad t_{min} = m_p^2 y - m_B^2 \frac{y}{1-y}. \quad (29)$$

In the above expressions x is the fraction of proton's momentum carried by the antiquark, and y is fraction carried by the meson (M). The meson-proton-baryon couplings are characterized by coupling constants g_{MpB} , and form factors $F_{MpB}(t, \Lambda)$ where Λ is a cutoff parameter. $F(t, m_p, m_B)$ is a kinematic factor depending on whether B is in the baryon octet or decuplet. As pions are the only mesons usually considered and the baryons are usually restricted to nucleons and deltas, the coupling constants are well known and the partonic structure of the pion, $\bar{q}_\pi(x, Q^2)$, is fixed by measurement of the DY process using high energy pion beams. The only uncertainties are the form factors $F_{\pi p N}(t)$ and $F_{\pi p \Delta}(t)$. One attempts to determine these form factors by using [121, 122] the measured yields from a variety of high

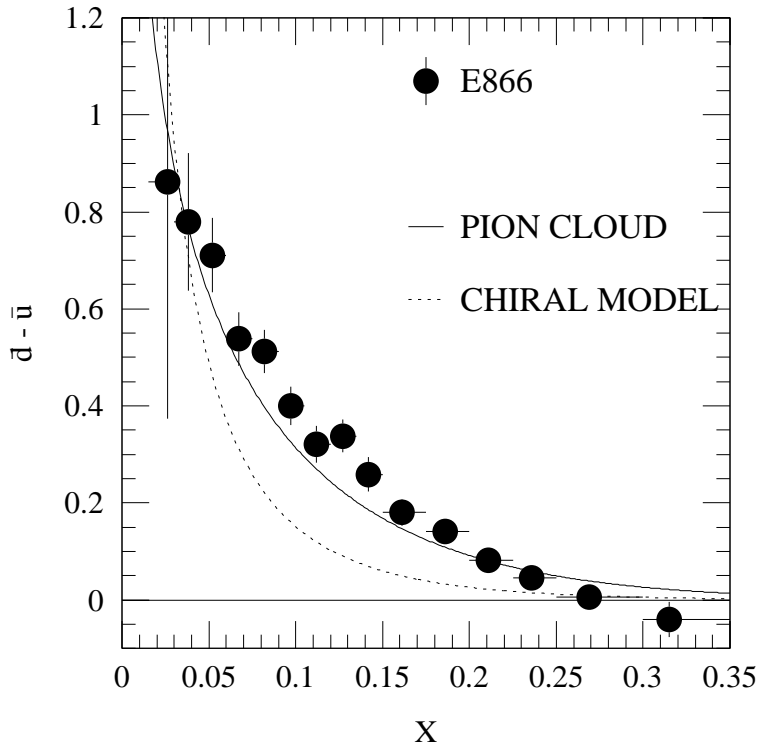


Figure 14: Comparison of the E866 [70] $\bar{d} - \bar{u}$ results at $Q^2 = 54 \text{ GeV}^2/c^2$ with the predictions of pion-cloud and chiral models as described in the text.

energy hadronic reactions at small p_T such as $pp \rightarrow nX$ and $pp \rightarrow \Delta^{++}X$. Even though there is a sizable amount of available data, employing such a procedure does not produce a precise result. The cutoff parameters used in the extracted form factors are of the order of 1 GeV but the uncertainties in their values produce factors of two in the predicted antiquark content of the nucleon due to pions.

Even though calculated value of the integral of $\bar{d}(x) - \bar{u}(x)$ is often in agreement with experiment, it is more difficult to achieve a quantitative fit to the measured x dependence of the difference [76]. Figure 14 compares $\bar{d}(x) - \bar{u}(x)$ from E866 with a pion-cloud model calculation, following the procedure detailed by Kumano [115]. A dipole form, with $\Lambda = 1.0 \text{ GeV}$ for the πNN form factor and $\Lambda = 0.8 \text{ GeV}$ for the $\pi N\Delta$ form factor, was used. Calculations of $\bar{d}(x)/\bar{u}(x)$ are even more unsuccessful, as knowledge of the x dependence of the symmetric sea is required in this instance [76].

It is instructive to compare the pion-model prediction with the current PDF parametrization of $x(\bar{d} + \bar{u})$. Figure 15 shows that at small x ($x < 0.1$) the valence quarks in the pion cloud account for less than 1/3 of the $\bar{d} + \bar{u}$ content in the proton. In contrast, at large x ($x > 0.5$) the pion model would attribute all of $\bar{d} + \bar{u}$ to the pion cloud.

Determining the appropriate cutoff is difficult because the high energy hadronic reactions ($pp \rightarrow \pi X$, $pp \rightarrow nX$, $pp \rightarrow \Delta^{++}X$) used to fix the form factors all have experimental backgrounds, and extracting quantitative results from such reactions is difficult. Nikolaev et al. [122] carefully investigated these reactions by including constraints from the Regge behavior of various mesons on the total photo-absorption cross section. They find that the contribution of ρ and a_2 Reggeons to the proton structure function is negligible. They also find the relative contribution of $\pi\Delta$ to be much smaller than previous analysis. For example $a = 0.105, b = 0.015$ for cutoffs of $R_G^2 = 1.5 \text{ GeV}^{-2}$ and $R_G^2 = 2 \text{ GeV}^{-2}$ for the πN and $\pi\Delta$ respectively. Their fits to $\bar{d}_p(x) - \bar{u}_p(x)$ are shown in Fig. 16.

In a recent publication [123] Thomas et al. appear to have avoided the form factor issue by having

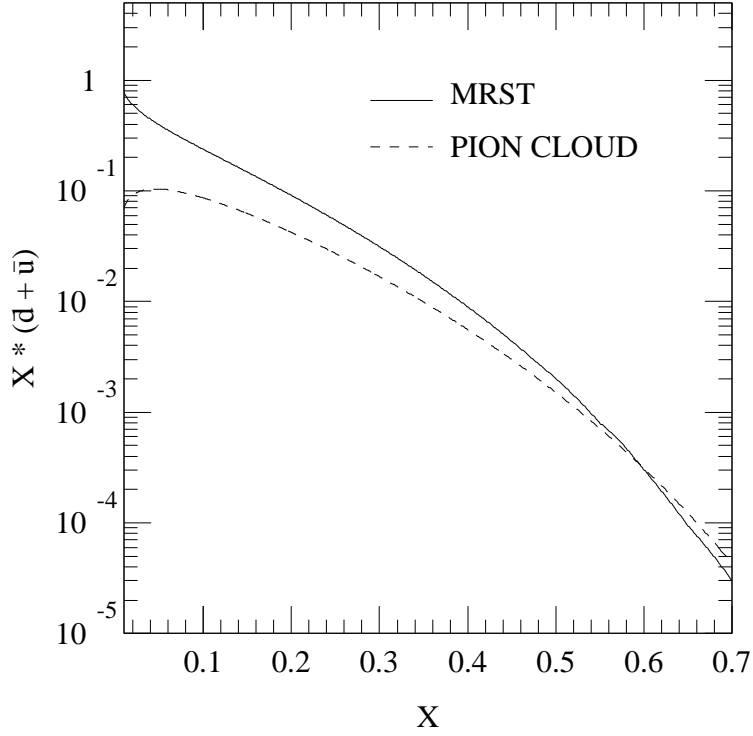


Figure 15: Comparison of $x(\bar{d} + \bar{u})$ obtained from the valence quarks in the pion cloud with the parametrization of the MRST parton distribution functions.

recourse to Chiral Perturbation Theory [124]. In this case the theory is implemented with pions, nucleons and deltas as the degrees of freedom. They find for the 0'th moment of the $\bar{d}_p(x) - \bar{u}_p(x)$ due to the πN loop to be

$$I_{AS}^{LNA}|_{\pi N} \equiv \int_0^1 dx [\bar{d}(x) - \bar{u}(x)] = \frac{2g_A^2}{(4\pi f_\pi)^2} m_\pi^2 \ln \frac{m_\pi^2}{\mu^2}, \quad (30)$$

where g_A is the axial charge of the nucleon, f_π the pion decay constant and μ a mass parameter. They stress that this leading non analytic (LNA) behavior originates from one-pion loop and hence is robust. General expressions are derived for the n'th order terms which are suppressed by powers of $(m_\pi/M_p)^n$. Using Eqs. (2), (5), (6) and (8) from Ref. [123] one obtains the ratio of the contribution of $\pi\Delta$ to that of πN to be

$$\frac{I_{AS}^{LNA}|_{\pi\Delta}}{I_{AS}^{LNA}|_{\pi N}} = -\frac{3}{75} \frac{(M_\Delta + M_N)^2}{M_\Delta^2} = -0.12. \quad (31)$$

Evaluating the net result using $\mu = 4\pi f_\pi$ one finds

$$I_{AS}^{LNA} = 0.154 \quad (32)$$

close to the E866 value of 0.118 ± 0.012 .

The values for I_{AS} that result from the various parametrizations of the πN and $\pi\Delta$ virtuality are all reasonable and not far from the experimentally measured value of 0.118 ± 0.012 . The values for a and b from various authors who have employed the meson cloud model show that a typical value of b/a is 1/2. This leads to $a = 0.24$, $b = 0.12$ to satisfy the observed flavor asymmetry, resulting in the probability of finding a pion in a nucleon (Eq. 25) of $a + b = 0.36$.

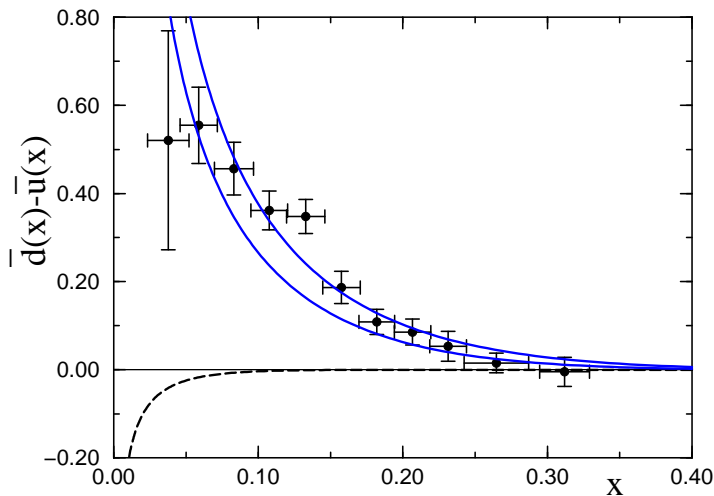


Figure 16: Flavor asymmetry at $Q^2 = 54 \text{ GeV}^2$. Experimental data are from E866 [70]. The solid curves are from Nikolaev et al. [122] for the πN Fock state with Gaussian form factors $R_G^2 = 1 \text{ GeV}^2$ (upper) and $R_G^2 = 1.5 \text{ GeV}^2$ (lower). The dashed line shows the contribution of the $\pi\Delta$ Fock state for a Gaussian form factor with $R_G^2 = 2 \text{ GeV}^2$.

The πN , $\pi\Delta$ model also allows one to evaluate the effect of virtual meson emission on the spin carried by quarks. The pion is emitted from the proton in a p -wave and therefore reduces the spin projection of the virtual baryon, thus reducing the spin projection carried by quarks. In this picture there is no spin on the antiquarks and the reduced spin in the baryon sector is carried off in the orbital motion of the pions. The expressions below for the spin on the quarks assumes an SU(6) wave function for the baryons.

$$\Delta u + \Delta d = 1 - \frac{2}{3}(2a - b) = 1 - 2I_{AS} \quad (33)$$

$$\Delta u - \Delta d = \frac{5}{3} - \frac{20}{27}(2a + b) + \frac{32}{27}\sqrt{2ab} \quad (34)$$

Where

$$\Delta q \equiv \int_0^1 [q(x) \uparrow + \bar{q}(x) \uparrow - q(x) \downarrow - \bar{q}(x) \downarrow] dx. \quad (35)$$

Interference occurs in Eq. 34 because the operator $\sigma_Z t_Z$ connects nucleon and delta states, while in Eq. 33 the operator σ_Z cannot. Thus, virtual pion emission is seen to reduce the spin carried by quarks. With no further assumptions we have $\Delta u + \Delta d = 0.76 \pm 0.024$, which is appreciably smaller than one but still greater than the observed value of 0.40 ± 0.02 . Employing a commonly used value of $b \simeq a/2$, we obtain $\Delta u - \Delta d = 1.51 \pm 0.053$. Again virtual pion emission reduces $\Delta u - \Delta d \equiv g_A$ from its SU(6) value of $5/3$ but not nearly to the measured value of 1.256 . Interestingly, the value extracted for g_A using the measured flavor asymmetry in this model is nearly identical to that obtained by Weinberg [125] using chiral perturbation theory and current algebra techniques.

4.3 Chiral Models

An alternative approach [66, 126, 127, 128, 129, 130, 131] also employing virtual pions to produce the \bar{d}, \bar{u} asymmetry is usually referred to as chiral models [101]. After the publication of the NMC

result on the violation of the Gottfried sum rule, Eichten, Hinchliffe and Quigg (EHQ) [66], following an earlier suggestion of Bjorken [132], published an interesting approach to explain the NMC result. They used chiral perturbation theory, employing the Manohar and Georgi [101] model in which the degrees of freedom are Goldstone Bosons (GB), and constituent quarks (i.e., U and D for up and down constituent quarks). The pion in this approach is emitted by a constituent quark. In this model most of the parameters are more or less prescribed (the mass of the constituent quark must be assigned). If α is the probability of a U constituent quark becoming π^+D , then to first order in α , invoking isospin invariance and the conservation of probability

$$U \rightarrow (1 - \frac{3}{2}\alpha)U + \alpha\pi^+D + \frac{1}{2}\alpha\pi^0U \quad (36)$$

with a corresponding expression for the down constituent quark. As the proton is UUD , to first order in α one has

$$p \rightarrow 2U + D + \frac{7\alpha}{4}(u + \bar{u}) + \frac{11\alpha}{4}(d + \bar{d}). \quad (37)$$

Thus the integrated asymmetry, I_{AB} , is equal to α . Note that in the absence of a symmetric sea the maximum value for $\bar{d}(x)/\bar{u}(x)$ in this model is 11/7. Restricting themselves to only the pion the authors calculate a value of $\alpha = 0.083$. This value is somewhat small, but within 50% of the measured value. However, it is very interesting that their calculation of α , carried out in the context of chiral field theory [101] generates a probability of finding a pion in a nucleon of $9\alpha/2 = 0.374$, very similar to that found in the meson-cloud model.

The authors also investigated the consequences of this model on the quark spins. Using SU(6) wave function for the proton and assuming total spin-flip of the constituent quark upon emitting a pion, they found for the modified quark spins in the proton

$$\Delta u + \Delta d = 1 - 3\alpha = 1 - 3I_{AS} \quad (38)$$

$$\Delta u - \Delta d = \frac{5}{3} - \frac{5}{3}\alpha. \quad (39)$$

Using $\alpha = 0.118 \pm 0.012$ from the E866 measured flavor asymmetry, $\Delta u + \Delta d = 0.65$ and $\Delta u - \Delta d = 1.47$. Both are reduced from the SU(6) values but are not as small as the measured values of 0.40 and 1.256, respectively. One believes that the SU(6) value is too large due to relativistic effects but the size of reduction is highly model dependent.

The differences that occur between the EHQ model and the meson-cloud model employed above are that the pion is emitted by a single constituent quark rather than by the proton. EHQ have a single parameter α which corresponds to fixing a/b at 5/4 in the meson-cloud model. We believe that this value is too small and does not easily produce the large values of $\bar{d}(x)/\bar{u}(x)$ that are observed in the interval $0.1 < x < 0.2$. EHQ achieves greater suppression of the quark spin because they assume a total spin flip of the constituent quark upon emission of a pion.

Reference [66] also examined the effect of extending the space of GBs beyond the pion. Treating the octet (π, K, η) of GBs as degenerate with equal coupling to all members, the proton becomes to first order in α' ,

$$p \rightarrow 2U + D + 2\alpha'(u + \bar{u}) + \frac{8}{3}\alpha'(d + \bar{d}) + \frac{10}{3}\alpha'(s + \bar{s}). \quad (40)$$

In this case the \bar{u}, \bar{d} flavor asymmetry is diluted, with the maximum value for $\bar{d}(x)/\bar{u}(x)$ becoming 1.333, and $I_{AS} = 2\alpha'/3$. Thus satisfying the E866 measured value for I_{AS} requires $\alpha' = 0.177 \pm 0.017$. The effect on the proton spin is given by

$$\Delta u - \Delta d = \frac{5}{3} - \frac{45\alpha'}{9} \quad (41)$$

$$\Delta u + \Delta d + \Delta s = 1 - \frac{16\alpha'}{3}. \quad (42)$$

Both larger value for α' and the larger number of mesons available to flip the quark spins conspire to produce a large effect on the spin values, $\Delta u - \Delta d = 0.978 \pm 0.066$ and $\Delta u + \Delta d + \Delta s = 0.056 \pm 0.091$. It is clear that this approach produces too little flavor asymmetry and too much reduction of quark spin. In addition one can see from Eq. 40 that far too much mesonic sea has to be generated to produce the observed flavor asymmetry. Continuing in this vein, EHQ showed that the \bar{u}, \bar{d} asymmetry vanishes in the case of an ideal U(3) nonet. This of course is not what is observed as the η and η' contributions are suppressed because they are much more massive than the π .

This approach has been considerably extended by Cheng and Li [126, 127, 133, 134] They employ the full meson U(3) nonet but allow the symmetry to be broken $U(3) \rightarrow SU(3) \times U(1)$. The coupling to the singlet η' is unique. Originally they made an ad hoc assumption that the singlet coupling was the negative of the octet coupling. Subsequently they have presented strong support for this point of view using the coupling of quarks to instantons [135, 136] and using the same physics that produces the large mass for the η' . Defining the ratio of the coupling to the singlet to that of the octet as $f_1/f_8 \equiv \zeta$, they found $\zeta = -2$. The ratio \bar{d}/\bar{u} in terms of ζ , due to the full nonet of GBs is

$$\frac{\bar{d}}{\bar{u}} = \frac{\frac{8}{3} + \frac{1}{3}\zeta^2}{2 + \frac{2}{3}\zeta + \frac{1}{3}\zeta^2}, \quad (43)$$

which gives 1 for $\zeta = 1$, and 4/3 for $\zeta = 0$ (the pure octet case). With $\zeta = -2$ the ratio is 2, an altogether reasonable value. However, in their most recent tabulation [134] of results they choose $\zeta = -1$ and generate the results shown in the third column of Table 3. In order to account for expected suppression factors arising from mass differences, they included a weighting factor, $(\langle k^2 \rangle + m_{GB}^2)^{-1}$, for each GB amplitude. This result is shown in column 4 and is seen to reduce the excessive contribution of strange quarks. This description while apparently quite successful, has the problem of producing a softer x distribution for $\bar{d}(x) - \bar{u}(x)$ than is observed in E866. Figure 14 shows a chiral-quark model calculation [76] using the formulation described in Ref. [129]. The predicted $\bar{d}(x) - \bar{u}(x)$ distribution is too soft because the GB is emitted by a constituent quark, which carries only 1/3 of the nucleon's momentum. This suggests that additional dynamics must be included in the chiral model if it is to produce agreement with the data.

Table 3: Comparison of the measured parton flavor and spin structure of the proton with the model of Cheng and Li [133, 134]. Some of the measured values are slightly different from the current values. The value of $\langle k^2 \rangle$ used is 350 MeV².

Quantity	Measured Value	SU3	Broken SU3
$\bar{d} - \bar{u}$	0.147 ± 0.026	0.15	0.15
$2\bar{s}/(\bar{u} + \bar{d})$	~ 0.5	1.86	0.6
Δu	0.82 ± 0.02	0.78	0.85
Δd	-0.43 ± 0.02	-0.33	-0.40
Δs	-0.10 ± 0.02	-0.11	-0.07
$\Delta \Sigma$	0.29 ± 0.06	0.34	0.38
$\Delta \bar{u}, \Delta \bar{d}$	0.01 ± 0.07	0.0	0.0
g_A	1.257 ± 0.03	1.12	1.25

By way of further comment on Table 3, there is no reason to expect the ratio of $2\bar{s}/(\bar{d} + \bar{u})$ generated from GBs alone should be 0.5, as this ratio depends sensitively on the contribution from the symmetric

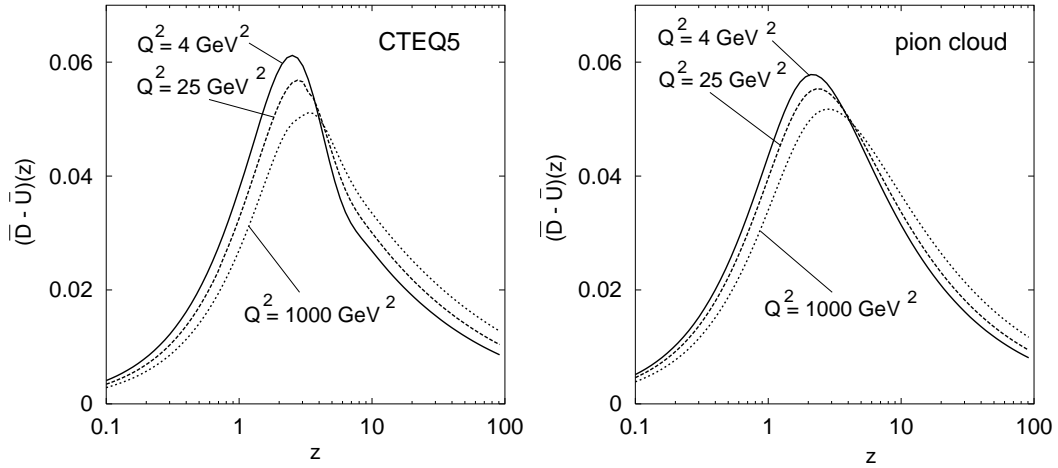


Figure 17: $(\bar{D} - \bar{U})(z)$ in coordinate space from CTEQ5 parton distributions and the pion cloud model [137].

sea. Also there is a lack of consistency in introducing a mass factor in the GB sector and ignoring the effect in the baryon sector. The baryons accompanying the GBs are $N, \Delta, \Lambda, \Sigma$ with mass splittings comparable to those occurring among the GB.

Continuing with approaches that explain the flavor asymmetry and spin quenching by introducing the role of mesons, a novel approach has been taken by Ball et al. [58, 59] in which the mesons are introduced by including them in the Q^2 evolution of the quark structure function functions as a non-singlet non-perturbative component. The approach is described in detail in [58, 59] and incorporates many attractive features. For example they explicitly account for the mass dependence of the contribution from each of the pseudoscalar mesons. Their approach generates a very strong scale dependence to the value observed for the Gottfried Sum Rule. Unfortunately, there is no relevant DIS data to verify their prediction. Drell-Yan experiments which could equivalently measure I_{AS} as a function of Q^2 are typically restricted to using lepton pairs above the Ψ' ($M_{\Psi'} = 3.69$ GeV), so have minimum Q^2 of ~ 16 GeV² making it impossible to observe the predicted scale dependence.

A very nice paper recently published by Henley, Renk, and Weise [137] showed that the distribution in x of $\bar{d}(x) - \bar{u}(x)$ measured by E866 corresponds to that associated with a pion cloud. Their result is somehow implicit in earlier work that showed the pion cloud model reproduced the x distribution observed in experiment, however this work makes explicit that the spatial distribution involved is what one would expect for a pion cloud. The method employed uses the coordinate space representation developed earlier by Piller et al. [138] and Vanttinen et al. [139]. They introduce a light-cone dimensionless space-time variable $z = y \cdot P$, where P is the nucleon momentum. The light-cone distance is $y^+ \equiv t + y_3 = 2z/M$, with M the nucleon mass. The dimensionless variable is conjugate to Bjorken x , and $z = 10$ corresponds to $y^+ = 4$ fm. The authors work with parton distribution functions such as CTEQ5 or MRST that accurately capture the measured $\bar{d}(x) - \bar{u}(x)$ distributions. The transformation from the x distribution is carried out via

$$(\bar{D} - \bar{U})(z, Q^2) \equiv \int_0^1 [\bar{d}(x, Q^2) - \bar{u}(x, Q^2)] \sin(zx) dx \quad (44)$$

Figure 17 shows how the $(\bar{D} - \bar{U})(z)$ distributions appear when plotted against z . The peak in z is at 2.5 or about 1fm and the bulk of the distribution is between $z = 1$ and 10 corresponding to 0.4 to 4 fm, in line with what one expects for a p -wave meson cloud.

4.4 Other Approaches not Directly Including Mesons

4.4.1 Instanton Models

Instantons have been known as theoretical constructs since the seventies [140, 141, 142]. They represent non-perturbative fluctuations of the gauge fields that induce transitions between degenerate ground states of different topology. In the case of QCD, the collision between a quark and an instanton flips the helicity of the quark while creating a $q\bar{q}$ pair of different flavor. Thus, interaction between a u quark and an instanton results in a u quark of opposite helicity and either a $d\bar{d}$ or $s\bar{s}$ pair. Such a model has the possibility of accounting for both the flavor asymmetry and the “spin crisis” [143, 144]. However, the model has proven difficult to exploit for this purpose. There is only one case [145] of its being directly employed to explain these anomalous effects. In the case of the \bar{d}, \bar{u} flavor asymmetry, the authors of ref. [145] fit the instanton parameters to reproduce the violation of the GSR observed by NMC. The prediction [145] at large x , $\bar{d}(x)/\bar{u}(x) \rightarrow 4$, is grossly violated by experiment (see Fig. 6). Thus, it appears that while instantons have the possibility for accounting for flavor and spin anomalies, the approach is not yet sufficiently developed for a direct comparison. The final state created via an instanton collision is quite similar to that created via the emission of meson in the chiral model.

However, it must be pointed out that the instanton model contains elements that strongly influence other descriptions. For example, as cited above in the work of Cheng et al. [135, 136], instantons provide the basis for generating a flavor asymmetry when the full GB nonet is employed. If the coupling to the η' is the same as the coupling to the GB octet, the sea is flavor symmetric. They originally made the ad hoc assumption that the η' coupling was equal in magnitude but opposite in sign to the coupling to the octet. This assumption has been justified [136] by invoking instantons. Further, as will be discussed below, the chiral quark soliton model which is developed using a vacuum sea of pions can equally well [146] be derived using the instanton model of the QCD vacuum. Thus it appears that the notion of instantons might be essential to the flavor asymmetry and that they play a crucial role in underpinning what ever explanation is used.

4.4.2 Lattice Gauge Approach

It would be extremely informative to explain the \bar{d}, \bar{u} asymmetry in terms of lattice gauge calculations as it would provide some insight as how the evolution of the asymmetry takes place. Indeed, soon after the existence of the asymmetry was established K.F. Liu and his collaborators investigated [147, 148] the issue. Employing a path-integral formalism they established that the \bar{d}, \bar{u} difference comes from the set of diagrams they termed connected diagrams (Fig. 18 (a,b)). The other sources of sea quarks are disconnected diagrams, shown in Fig. 18(c). The loops in the disconnected diagrams are generated by gluons, and can produce all flavors of sea quarks. These diagrams produce equal numbers of up and down sea quarks. The loops in the connected diagrams can only produce up and down sea quarks and presumably are the source of the up, down asymmetry.

This approach has the interesting feature that the strange quark sea is created entirely from disconnected diagrams and hence the s and \bar{s} distributions are identical, in good agreement with the results from neutrino DIS. It would also account for the near vanishing of the strange vector form factors for the nucleon as extracted from parity violating electron scattering. However it leaves unspecified the spin carried by strange quarks.

4.4.3 Chiral-Quark Soliton Model

One of the interesting approaches to emerge over the past 5 years is that of the chiral-quark soliton model [146, 149, 150, 151, 152]. It uses the large N_c limit of QCD, which becomes an effective theory of mesons with the baryons appearing as solitons. At low energy the effective dynamics is described by a

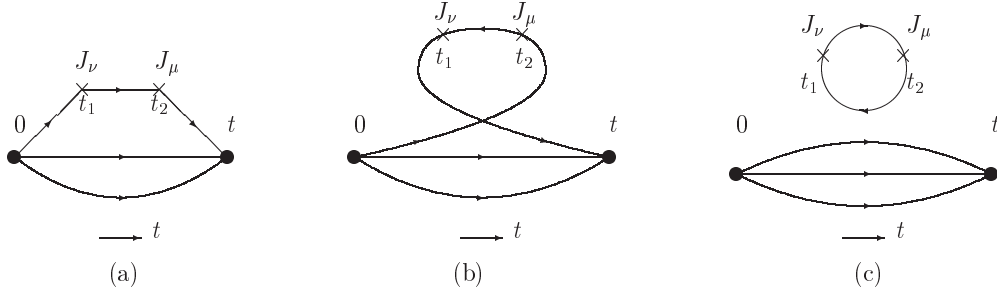


Figure 18: Euclidean path integral from Ref. [148] for evaluating the hadronic tensor $W_{\nu\mu}$. (a) and (b) are connected insertions and (c) is a disconnected insertion.

chiral Lagrangian for the pion, which appears as the GB of the spontaneously broken chiral symmetry. The model employs a realistic effective interaction, containing all orders of derivatives of the pion field, defined by the integral over quark fields having dynamically generated mass and interacting with the pion field in a minimally chirally invariant way. It is valid over a range of momenta up to the inverse of the instanton size ($1/\rho = 0.6$ GeV). The parton distribution obtained at this low momentum scale can then be evolved to higher Q^2 for comparison to experiment.

Quarks are described by single particle wave functions which are solutions of the Dirac equation in the field of the background pions. The spectrum of single particle states includes a single bound state level plus distorted positive and negative Dirac continuum. The discrete level and the negative continuum are occupied producing a state of unit baryon number. The distribution $\Delta\bar{u}(x) - \Delta\bar{d}(x)$ appears in leading order (N_c^2) in a $1/N_c$ expansion while $\bar{u}(x) - \bar{d}(x)$ appears in next-to-leading order. For example the isovector spin carried by quarks is

$$\Delta u(x) - \Delta d(x) = -\frac{1}{3}(2T_3)N_c M_N \sum_{n(\text{occup})} \int \frac{d^3k}{(2\pi)^3} \tilde{\Psi}_n^*(\mathbf{k})(1 + \gamma^0\gamma^3)\gamma_5\tau^3\delta(k_3 + E_n + xM_n)\Psi_n(\mathbf{k}). \quad (45)$$

Where $\Psi_n(\mathbf{k})$ are the single particle wave functions, and $2T_3 = \pm 1$ for the proton and neutron respectively. The sum runs over all occupied single particle quark states, the bound state and the negative continuum. Figure 19 shows some of the results from Ref. [153].

The values for the integral of the quantities shown in Fig. 19 are

$$\int_0^1 [\bar{d}(x) - \bar{u}(x)]dx = 0.17; \quad \int_0^1 [\Delta\bar{d}(x) - \Delta\bar{u}(x)]dx = -0.31. \quad (46)$$

Equation 46 presents a value for the integrated flavor asymmetry that is larger, but in the same ballpark as the measured value (0.118 ± 0.012). The distribution in x is not unlike that of models employing virtual mesons and hence should have a similar spatial distribution. However, the magnitude of the integrated isovector longitudinal-spin distribution for the antiquarks is surprisingly large and totally at variance with the results of models employing GBs to account for the flavor asymmetry. The GB models obviously require $\Delta\bar{d}(x) = \Delta\bar{u}(x) = 0$. While one might think that the chiral soliton model should be consistent with the GB models as the baryonic soliton is developed in a background field of pions, the result for the spin carried by the antiquarks is totally at odds with any GB description. Hence one cannot view this non-perturbative approach as generating pseudoscalar mesons. Recent data [86]

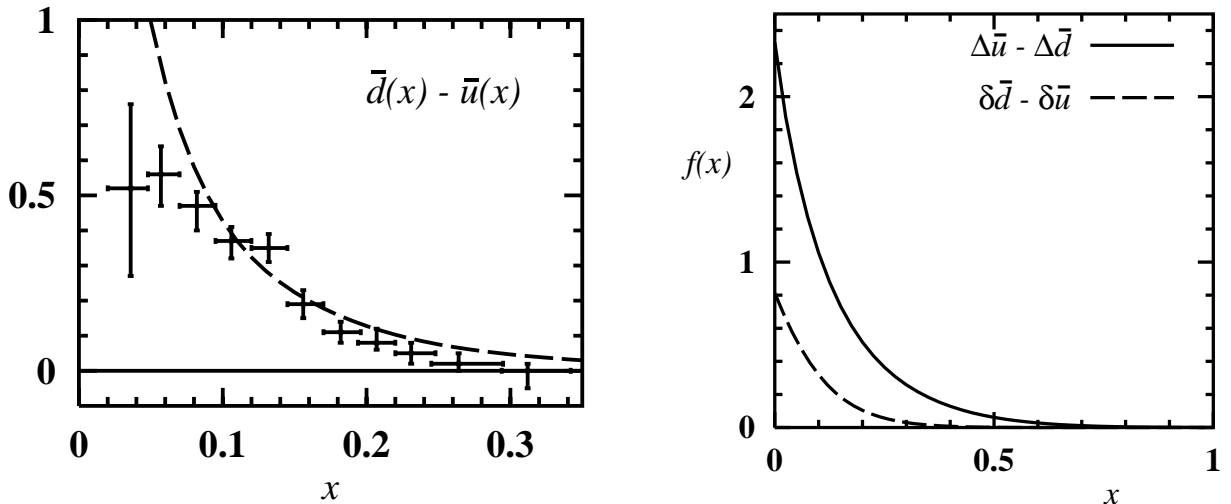


Figure 19: Calculations from a chiral-quark soliton model [153] (a) The value calculated for $\bar{d}(x) - \bar{u}(x)$ in the proton compared to early data from E866. The calculation has been evolved from $Q = 0.6$ GeV to $Q = 7.35$ GeV. (b) The calculated flavor asymmetry of the longitudinally polarized antiquark distribution in the proton (solid line) and the transversity distribution of the antiquarks (dashed line). Both distributions are at $Q = 0.6$ GeV.

showed $\Delta\bar{q} = 0.01 \pm 0.04 \pm 0.03$, consistent with a small sea polarization. We await the judgement of future experiments to decide which description best conforms to reality.

5 Further Implications of the Meson-Cloud Models

5.1 Strange Sea of the Nucleon

Models in which virtual mesons are admitted as degrees of freedom have implications that extend beyond the \bar{d}, \bar{u} flavor asymmetry addressed above. They create hidden strangeness in the nucleon via such virtual processes as $p \rightarrow \Lambda + K^+, \Sigma + K$, etc. Such processes are of considerable interest as they imply different s and \bar{s} parton distributions in the nucleon, a feature not found in gluonic production of $s\bar{s}$ pairs. This subject has received a fair amount of attention in the literature [121, 154, 155, 156, 157] but experiments have yet to clearly identify such a difference. Thus in contrast to the \bar{d}, \bar{u} flavor asymmetry, to date there is no positive experimental evidence for $s\bar{s}$ contributions to the nucleon from virtual meson-baryon states [19, 158].

A difference between the s and \bar{s} distribution can be made manifest by direct measurement of the s and \bar{s} parton distribution functions in DIS neutrino scattering, or in the measurement of the q^2 dependence of the strange quark contribution ($F_{1s}^p(q^2)$) to the proton charge form factor. This latter case is not well known and follows from a suggestion of Kaplan and Manohar [159] regarding the new information contained in the weak neutral current form factors of the nucleon. Measurement of these form factors allows extraction of the strangeness contribution to the nucleon's charge and magnetic moment and axial form factors. The portion of the charge form factor $F_{1s}^p(q^2)$ due to strangeness

clearly is zero at $q^2 = 0$, but if the s and \bar{s} distributions are different the form factor becomes non-zero at finite q^2 . These “strange” form factors can be measured in neutrino elastic scattering [160] from the nucleon, or by selecting the parity-violating component of electron-nucleon elastic scattering, as is now being done at the Bates [161] and Jefferson Laboratories [162].

It is worth pointing out that there is a relationship between the parton distributions and the form factors of a hadron. If the neutron’s charge form factor is explained in terms of a particular meson-baryon expansion, then one should expect that the expansion is consistent with the neutron’s partonic structure. Little work appears to have been done bringing these descriptions together. Below is an example showing the impact of the nucleon’s pionic content, inferred from the flavor asymmetry, on the spin distribution in the nucleon.

5.2 Sea Quark Distributions in Hyperons

Dilepton production using meson or hyperon beams offers a means of determining parton distributions of these unstable hadrons. Many important features of nucleon parton distributions, such as the flavor structure and the nature of the non-perturbative sea, find their counterparts in mesons and hyperons. Information about meson and hyperon parton structure could provide valuable new insight into nucleon parton distributions. Furthermore, certain aspects of the nucleon structure, such as the strange quark content of the nucleon, could be probed with kaon beams.

No data exist for hyperon-induced dilepton production. The observation of a large \bar{d}/\bar{u} asymmetry in the proton has motivated Alberg et al. [163, 164] to consider the sea-quark distributions in the Σ . The meson-cloud model implies a \bar{d}/\bar{u} asymmetry in the Σ^+ even larger than that of the proton. However, the opposite effect is expected from SU(3) symmetry. Although relatively intense Σ^+ beams have been produced for recent experiments at Fermilab, this experiment appears to be very challenging because of large pion, kaon, and proton contaminations in the beam.

6 Future Prospects

6.1 \bar{d}/\bar{u} at Large and Small x

The interplay between the perturbative and non-perturbative components of the nucleon sea remains to be better determined. Since the perturbative process gives a symmetric \bar{d}/\bar{u} while a non-perturbative process is needed to generate an asymmetric \bar{d}/\bar{u} sea, the relative importance of these two components is directly reflected in the \bar{d}/\bar{u} ratios. Thus, it would be very important to extend the DY measurements to kinematic regimes beyond the current limits.

The new 120 GeV Fermilab Main Injector (FMI) and the proposed 50 GeV Japanese Hadron Facility [165] (JHF) present opportunities for extending the \bar{d}/\bar{u} measurement to larger x ($x > 0.25$). For given values of x_1 and x_2 the DY cross section is proportional to $1/s$, hence the DY cross section at 50 GeV is roughly 16 times greater than that at 800 GeV! Figure 20 shows the expected statistical accuracy for $\sigma(p+d)/2\sigma(p+p)$ at JHF [166, 167] compared with the data from E866 and a proposed measurement [168] using the 120 GeV proton beam at the FMI. A definitive measurement of the \bar{d}/\bar{u} over the region $0.25 < x < 0.7$ could indeed be obtained at FMI and JHF.

At the other end of the energy scale, RHIC will operate soon in the range $50 \leq \sqrt{s} \leq 500$ GeV/nucleon. The capability of accelerating and colliding a variety of beams from $p+p$, $p+A$, to $A+A$ at RHIC offers a unique opportunity to extend the DY \bar{d}/\bar{u} measurement to very small x . Such information is important for an accurate determination of the integral of $\bar{d} - \bar{u}$, as well as for a better understanding of the origins for flavor asymmetry. The statistical accuracy for measuring $\sigma(p+d)/2\sigma(p+p)$ in a two-month PHENIX run is shown in Fig. 21. Also shown in Fig. 21 are the

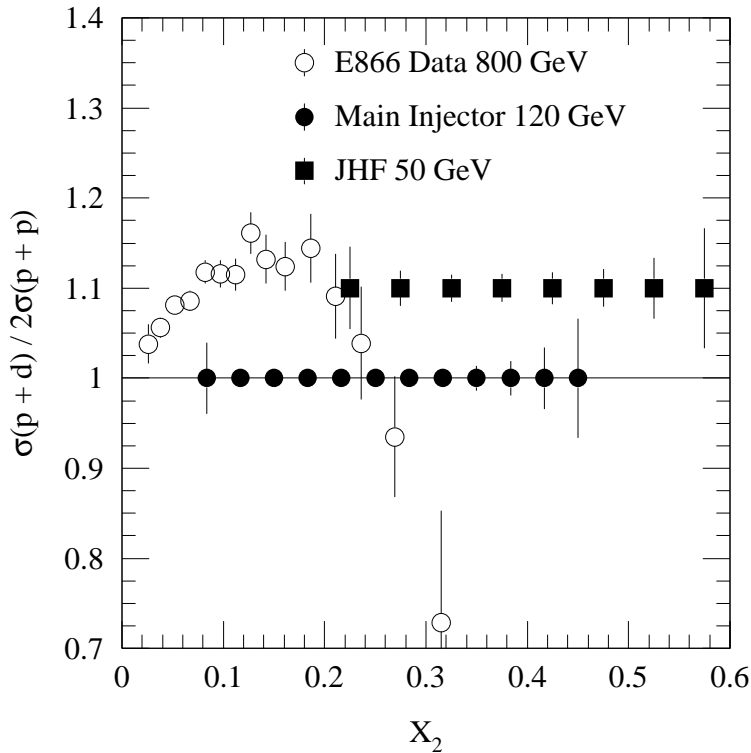


Figure 20: Projected statistical accuracy for $\sigma(p+d)/2\sigma(p+p)$ in a 100-day run at JHF [166, 167]. The E866 data and the projected sensitivity for a proposed measurement [168] at the 120 GeV Fermilab Main-Injector are also shown.

data from E866. The lowest x_2 reachable at RHIC is around 10^{-3} , an order of magnitude lower than in E866.

6.2 W Production

To disentangle the \bar{d}/\bar{u} asymmetry from the possible charge-symmetry violation effect [169, 170, 171], one could consider W boson production, a generalized DY process, in $p+p$ collision at RHIC. An interesting quantity to be measured is the ratio of the $p+p \rightarrow W^+ + X$ and $p+p \rightarrow W^- + X$ cross sections [172]. It can be shown that this ratio is very sensitive to \bar{d}/\bar{u} . An important feature of the W production asymmetry in $p+p$ collision is that it is completely free from the assumption of charge symmetry. Figure 22 shows the predictions for $p+p$ collision at $\sqrt{s} = 500$ GeV. The dashed curve corresponds to the \bar{d}/\bar{u} symmetric MRS S0' [173] structure functions, while the solid and dotted curves are for the \bar{d}/\bar{u} asymmetric structure function MRST and MRS(R2), respectively. Figure 22 clearly shows that W asymmetry measurements at RHIC could provide an independent determination of \bar{d}/\bar{u} .

6.3 Strange Sea in the Nucleon

As discussed earlier, an interesting consequence of the meson-cloud model is that the s and \bar{s} distributions in the proton could have very different shapes, even though the net amount of strangeness in the proton vanishes. By comparing the ν and $\bar{\nu}$ induced charm production, the CCFR collaboration found no difference between the s and \bar{s} distributions [158]. More precise future measurements would be very helpful. Dimuon production experiments using K^\pm beams might provide an independent

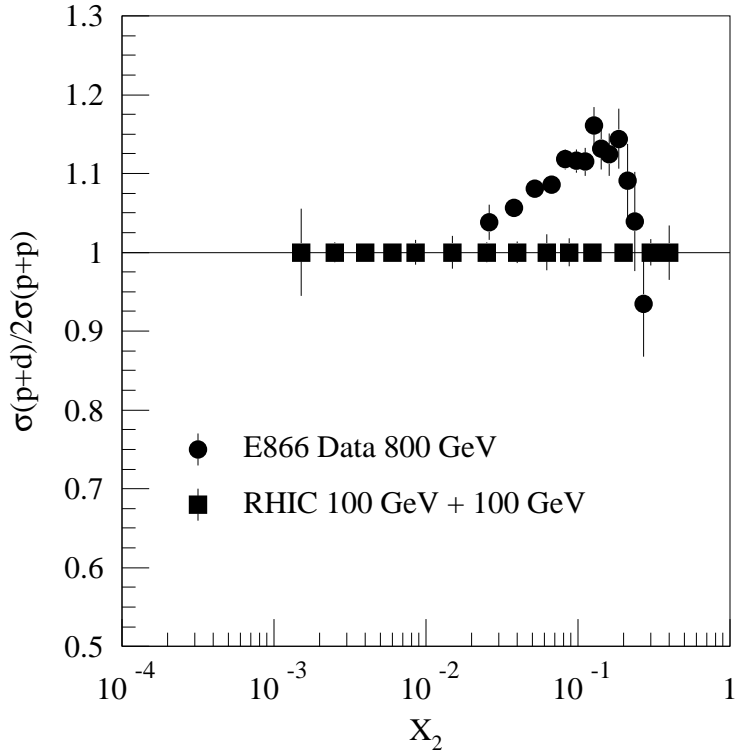


Figure 21: Projected statistical accuracy for $\sigma(p+d)/2\sigma(p+p)$ in a two-month run at RHIC using the PHENIX detector [183]. The E866 data are also shown.

determination of the s/\bar{s} ratio of the proton, provided that our current knowledge on valence-quark distributions in kaons is improved. As discussed in Section 5.1, ongoing measurements of F_{1s}^p via parity-violating electron-nucleon scattering should shed much light on the possible difference between s and \bar{s} distributions.

6.4 Sea Quark Polarization

Polarized DY and W^\pm production in polarized $p+p$ collision are planned at RHIC [174] and they have great potential for providing qualitatively new information about antiquark polarization. At large x_F region ($x_F > 0.2$), the longitudinal spin asymmetry A_{LL} in the $p+p$ DY process is given by [175, 176]

$$A_{LL}^{DY}(x_1, x_2) \approx g_1(x_1)/F_1(x_1) \times \frac{\Delta\bar{u}}{\bar{u}}(x_2), \quad (47)$$

where $g_1(x)$ is the proton polarized structure function measured in DIS, and $\Delta\bar{u}(x)$ is the polarized \bar{u} distribution function.

Equation 47 shows that \bar{u} polarization can be determined using polarized DY at RHIC. Additional information on the sea-quark polarization can be obtained via W^\pm production [177]. The parity-violating nature of W production implies that only one of the two beams need to be polarized. At positive x_F (along the direction of the polarized beam), one finds[177],

$$A_L^{W^+} \approx \frac{\Delta u}{u}(x_2), \quad \text{and} \quad A_L^{W^-} \approx \frac{\Delta d}{d}(x_2), \quad (48)$$

where A_L^W is the single-spin asymmetry for W production. Equation 48 shows that the flavor dependence of the sea-quark polarization can be revealed via W^\pm production at RHIC. A remarkable prediction of

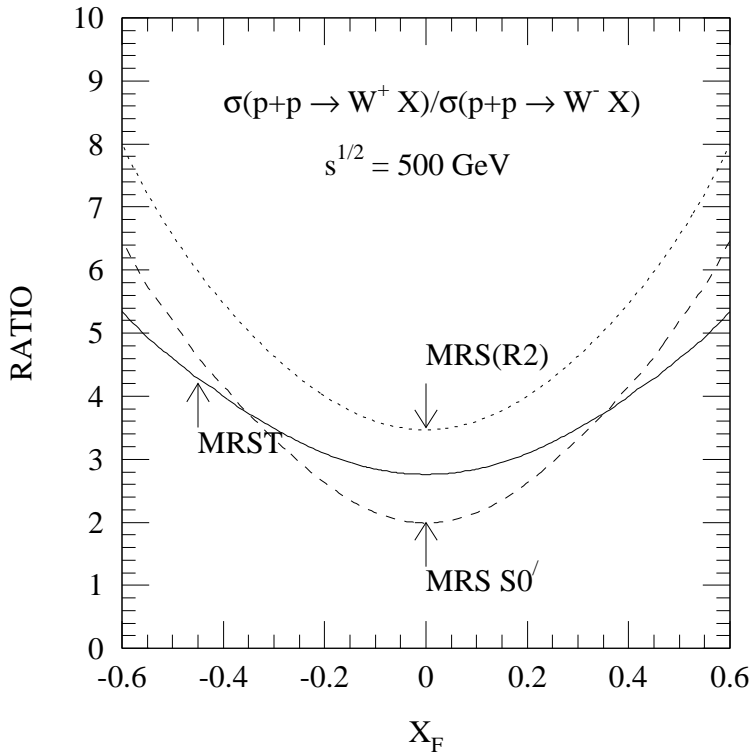


Figure 22: Predictions of $\sigma(p+p \rightarrow W^+ X)/\sigma(p+p \rightarrow W^- X)$ as a function of x_F at $\sqrt{s} = 500$ GeV. The dashed curve corresponds to the \bar{d}/\bar{u} symmetric MRS S0' structure functions, while the solid and dotted curves are for the \bar{d}/\bar{u} asymmetric structure function MRST and MRS(R2), respectively.

the chiral quark-soliton model is that the flavor asymmetry of polarized sea-quark, $\Delta\bar{u}(x) - \Delta\bar{d}(x)$, is very large [178]. This is in striking contrast to the meson cloud model which predicts very small values for $\Delta\bar{u}(x) - \Delta\bar{d}(x)$ [179, 180]. Future DY and W^\pm production experiments at RHIC could clearly test these models [181]

6.5 Hard Processes Tagged by Leading Particles

The role of the meson-cloud model in explaining the \bar{d}/\bar{u} asymmetry suggests a novel technique to study meson substructures without using a meson beam. The idea is that the meson cloud in the nucleon could be considered as a virtual target to be probed by various hard processes. Recently at the HERA e-p collider, meson structure functions were measured in a hard diffractive process, where forward-going neutrons or protons were tagged in coincidence with the DIS events [182]. Analogous measurements could be done at RHIC for p-p collisions [183]. In particular, a DY pair in coincidence with a forward-going neutron or proton could provide information on the antiquark distributions in pions at small x . The underlying picture of the tagged DY process is as follows. A proton fluctuates into a baryon plus a meson ($p \rightarrow n + \pi^+$, $p \rightarrow \Lambda + K^+$, for example) and the other proton beam interacts with the meson, producing a lepton pair. The remaining baryon moves roughly along the initial proton beam direction and could be detected at forward angles. A simulation for the $p+p \rightarrow n + \mu^+\mu^- + X$ for the PHENIX detector, where the muon pairs are detected in the muon arms and the neutrons are detected by a small-angle calorimeter showed that such measurement is quite feasible [183].

Drell-Yan experiment tagged by forward-going baryons at RHIC would provide a direct test of the

meson-cloud model. One could also conceive tagging forward-going Δ or Λ . The Λ -tagging is of special interest since it can shed light on the strange-quark contents of the proton. Another extension is the measurement of double-helicity asymmetry, A_{LL} , in neutron-tagged $\vec{p} + \vec{p}$ Drell-Yan process. If the dominant underlying process is $\vec{p} + \pi$ interaction, A_{LL} is expected to be zero.

7 Conclusion

The flavor asymmetry of the nucleon sea has been clearly established by recent DIS and DY experiments. The surprisingly large asymmetry between \bar{u} and \bar{d} is unexplained by perturbative QCD. We draw the following conclusions:

- The x dependence of \bar{d}_p/\bar{u}_p indicates that a \bar{d}, \bar{u} symmetric sea dominates at small ($x < 0.05$) and large x ($x > 0.3$). But for $0.1 < x < 0.2$ a large and significant flavor non-symmetric contribution determines the sea distributions.
- The value of the integrals

$$\int_0^1 [\bar{d}_p(x, Q^2) - \bar{u}_p(x, Q^2)] dx = \int_0^1 [\bar{u}_n(x, Q^2) - \bar{d}_n(x, Q^2)] dx = 0.118 \pm 0.012 \quad (49)$$

are approximately independent of Q^2 and are characteristic of the nucleon.

- The value of the integral and the distribution in x can be reproduced using virtual pions. The x distribution favors the virtual pion being emitted by the nucleon as a whole, rather than by a constituent quark.
- Virtual pion emission reduces the spin carried by quarks but is not sufficient to account for the observed reduction.
- The mean square charge in the neutron sea is less than that in the proton sea, because $\bar{u}_n > \bar{d}_n$ and $\bar{d}_p > \bar{u}_p$.

The up-down flavor asymmetry in the nucleon sea is as fundamental as the axial vector coupling constant, g_A , in characterizing the properties of the nucleon. This asymmetry is of a completely non-perturbative origin but, differently from g_A , could only be observed by measurements at the partonic level. Thus it stands as a key property of the nucleon that awaited the discovery of perturbative QCD processes and the associated high-energy facilities to uncover it. While the nucleon “spin crisis” involves both perturbative (spin carried by gluons) and non-perturbative processes (spin flips due to the emission of virtual GBs), the origin of the up-down asymmetry in the nucleon sea is entirely non-perturbative. Fortunately, it is most likely that the origin of this asymmetry lies with the presence of virtual isovector mesons, mostly pions, in the nucleon sea. The unfortunate aspect of this problem is that 70 years of research in nuclear physics and the structure of the nucleon is still unable to provide a quantitative answer to this basic question. Probably a clear picture would eventually emerge after some future experimental investigation which includes:

- Measurement of \bar{d}_p/\bar{u}_p for $x > 0.25$ and $x < 0.01$ to more firmly establish the origin of the flavor asymmetry.
- $\Delta\bar{d}$ and $\Delta\bar{u}$ in the interval $0.1 < x < 0.2$ needs to be measured. Each must be ~ 0 if the pionic explanation of the \bar{d}, \bar{u} asymmetry is correct. The chiral soliton model predicts that $\Delta\bar{d} - \Delta\bar{u} \sim -0.5$ in the proton for this x interval.

- Semi-inclusive including polarized DIS and Drell-Yan experiments to demonstrate the role of mesonic degrees of freedom in the nucleon's makeup.
- More precise measurements on the s versus \bar{s} distributions in the nucleon.
- Experimental identification of instantons.

Acknowledgment

We are grateful to our collaborators on the Fermilab E772 and E866. This work was supported by the US Department of Energy, Nuclear Science Division, under contract W-7405-ENG-36.

References

- [1] E. D. Bloom et al., Phys. Rev. Lett. **23** (1969) 930.
- [2] M. Breidenbach et al., Phys. Rev. Lett. **23** (1969) 935.
- [3] R. P. Feynman, Photon-Hadron Interactions (Benjamin, New York, 1972).
- [4] K. F. Liu et al., Phys. Rev. **D59** (1999) 112001.
- [5] J. D. Bjorken, Phys. Rev. **179** (1969) 1547.
- [6] R. P. Feynman, Phys. Rev. Lett. **23** (1969) 1415.
- [7] S. D. Drell, D. J. Levy and T. M. Yan, Phys. Rev. **187** (1969) 2159.
- [8] S. D. Drell, D. J. Levy and T. M. Yan, Phys. Rev. **D1** (1970) 1035; **D1** (1970) 1617.
- [9] N. G. Cabbibo, G. Parisi, M. Testa and A. Verganelakis, Lett. Nuovo Cimento **4** (1970) 569.
- [10] T. D. Lee and S. D. Drell, Phys. Rev. **D5** (1972) 1738.
- [11] J. D. Bjorken and E. A. Paschos, Phys. Rev. **185** (1969) 1975.
- [12] J. Kuti and V. F. Weisskopf, Phys. Rev. **D4** (1971) 3418.
- [13] P. V. Landschoff and J. C. Polkinghorne, Nucl. Phys. **B28** (1971) 240.
- [14] M. Gell-Mann, Phys. Lett. **8** (1964) 214.
- [15] G. Zweig, CERN Preprint 8182/TH401, 8419/TH412 (1964).
- [16] J. I. Friedman and H. W. Kendall, Annu. Rev. Nucl. Sci. **22** (1972) 203.
- [17] J. G. H. de Groot et al., Z. Phys. **C1** (1979) 143.
- [18] H. Abromowicz et al., Z. Phys. **C15** (1982) 19.
- [19] J. M. Conrad, M. H. Shaevitz and T. Bolton, Rev. Mod. Phys. **70** (1998) 1341.
- [20] K. Gottfried, Phys. Rev. Lett. **18** (1967) 1174.
- [21] J. D. Bjorken, Proc. 1967 Int. Sym. on Electron and Photon Interactions at High Energies, Stanford, CA (1967) 109.
- [22] E. D. Bloom et al., Proc. 15th Int. Conf. on High Energy Phys., Kiev, USSR (1970).
- [23] E. D. Bloom, Proc. 6th Int. Sym. on Electron and Photon Interactions at High Energies, edited by H. Rollnik and W. Pfeil (North-Holland, Amsterdam, 1974) 227.
- [24] R. D. Field and R. P. Feynman, Phys. Rev. **D15** (1977) 2590.
- [25] Y. Watanabe et al., Phys. Rev. Lett. **35** (1975) 898.
- [26] C. Chang et al., Phys. Rev. Lett. **35** (1975) 901.
- [27] B. A. Gordon et al., Phys. Rev. **D20** (1979) 2645.

- [28] J. J. Aubert et al., Nucl. Phys. **B293** (1987) 740.
- [29] A. C. Benvenuti et al., Phys. Lett. **B237** (1990) 599.
- [30] A. Bodek et al., Phys. Rev. **D20** (1979) 1471.
- [31] D. W. Duke and J. F. Owens, Phys. Rev. **D30** (1984) 49.
- [32] E. Eichten, I. Hinchliffe, K. Lane and C. Quigg, Rev. Mod. Phys. **56** (1984) 579; Rev. Mod. Phys. **58** (1985) 1065.
- [33] M. Diemoz, F. Ferroni, E. Longo and G. Martinelli, Z. Phys. **C39** (1988) 21.
- [34] A. D. Martin, R. G. Roberts and W. J. Stirling, Phys. Lett. **B206** (1988) 327.
- [35] P. Aurenche et al., Phys. Rev. **D39** (1989) 3275.
- [36] J. H. Christensen et al., Phys. Rev. Lett. **25** (1970) 1523.
- [37] S. D. Drell and T. M. Yan, Phys. Rev. Lett. **25** (1970) 316.
- [38] S. W. Herb et al., Phys. Rev. Lett. **39** (1977) 252.
- [39] D. M. Kaplan et al., Phys. Rev. Lett. **40** (1977) 435.
- [40] A. S. Ito et al., Phys. Rev. **D23** (1981) 604.
- [41] S. R. Smith et al., Phys. Rev. Lett. **46** (1981) 1607.
- [42] J. J. Aubert et al., Phys. Lett. **B123** (1983) 295.
- [43] J. Ashman et al., Phys. Lett. **B202** (1988) 603.
- [44] D. Allasia et al., Phys. Lett. **B249** (1990) 366.
- [45] P. Amaudruz et al., Nucl. Phys. **B441** (1995) 3.
- [46] P. Amaudruz et al., Phys. Rev. Lett. **66** (1991) 2712.
- [47] L. W. Whitlow et al., Phys. Lett. **B282** (1992) 475.
- [48] A. C. Benvenuti et al., Phys. Lett. **B237** (1990) 592.
- [49] M. Arneodo et al., Nucl. Phys. **B333** (1990) 1.
- [50] M. Arneodo et al., Phys. Rev. **D50** (1994) R1.
- [51] P. Amaudruz et al., Phys. Lett. **B295** (1992) 159.
- [52] M. Arneodo et al., Nucl. Phys. **B487** (1997) 3.
- [53] M. Arneodo et al., Phys. Lett. **B364** (1995) 107.
- [54] M. Arneodo et al., Nucl. Phys. **B483** (1997) 3.
- [55] I. Hinchliffe and A. Kwiatkowski, Annu. Rev. Nucl. Part. Sci. **46** (1996) 609.
- [56] D. A. Ross and C. T. Sachrajda, Nucl. Phys. **B149** (1979) 497.
- [57] A. L. Kotaev, A. V. Kotikov, G. Parente, and A. V. Sidorov, Phys. Lett. **B388** (1996) 179.
- [58] R. D. Ball and S. Forte, Nucl. Phys. **B425** (1994) 516.
- [59] R. D. Ball, V. Barone, S. Forte, and M. Genovese, Phys. Lett. **B329** (1994) 505.
- [60] D. F. Geesaman, K. Saito and A. W. Thomas, Annu. Rev. Nucl. Part. Sci. **45** (1995) 337.
- [61] C. H. Llewellyn-Smith, Phys. Lett. **B128** (1983) 107; M. Ericson and A. W. Thomas, Phys. Lett. **B128** (1983) 112; E. L. Berger, F. Coester and R. B. Wiringa, Phys. Rev. **D29** (1984) 398.
- [62] D. M. Alde et al., Phys. Rev. Lett. **64** (1990) 2479.
- [63] F. E. Close, R. L. Jaffe, R. G. Roberts and G. G. Ross, Phys. Rev. **D31** (1985) 1004.
- [64] P. L. McGaughey et al., Phys. Rev. Lett. **69** (1991) 1726.
- [65] S. D. Ellis and W. J. Stirling, Phys. Lett. **B256** (1991) 258.
- [66] E. Eichten, I. Hinchliffe and C. Quigg, Phys. Rev. **D45** (1992) 2269.

- [67] A. D. Martin, R. G. Roberts, W. J. Stirling and R. S. Thorne, Eur. Phys. J. **C4** (1998) 463.
- [68] S. Kumano, Phys. Lett. **B342** (1995) 339.
- [69] A. Baldit et al., Phys. Lett. **B332** (1994) 244.
- [70] E. A. Hawker et al., Phys. Rev. Lett. **80** (1998) 3715.
- [71] R. S. Towell et al., hep-ex/0103030 (2001).
- [72] H. L. Lai et al., Phys. Rev. **D55** (1997) 1280.
- [73] A. D. Martin, R. G. Roberts and W. J. Stirling, Phys. Lett. **B387** (1996) 419.
- [74] H. L. Lai et al., Eur. Phys. J. **C12** (2000) 375.
- [75] M. Glück, E. Reya and A. Vogt, Eur. Phys. J. **C5** (1998) 461.
- [76] J. C. Peng et al., Phys. Rev. **D58** (1998) 092004.
- [77] M. Gronau, F. Ravndal and Y. Zarmi, Nucl. Phys. **B51** (1973) 611.
- [78] J. Ashman et al., Z. Phys. **C52** (1991) 361.
- [79] D. Allasia et al., Phys. Lett. **B135** (1984) 231.
- [80] H. Abramowicz et al., Z. Phys. **C25** (1984) 29.
- [81] J. Levelt, P. J. Mulders and A. W. Schreiber, Phys. Lett. **B263** (1991) 498.
- [82] K. Ackerstaff et al., Phys. Rev. Lett. **81** (1998) 5519.
- [83] M. Glück, E. Reya and A. Vogt, Z. Phys. **C67** (1995) 433.
- [84] L. L. Frankfurt et al., Phys. Lett. **B230** (1989) 141.
- [85] F. E. Close and R. G. Milner, Phys. Rev. **D44** (1991) 3691.
- [86] B. Adeva et al., Phys. Lett. **B369** (1997) 93; B. Adeva et al., Phys. Lett. **B420** (1998) 180.
- [87] K. Ackerstaff et al., Phys. Lett. **B464** (1999) 123.
- [88] H. L. Lai, private communication (1999).
- [89] F. Abe et al., Phys. Rev. Lett. **81** (1998) 5754.
- [90] R. D. Ball et al., Phys. Lett. **B329** (1994) 505.
- [91] F. M. Steffens and A. W. Thomas, Phys. Rev. **C55** (1997) 900.
- [92] D. A. Dicus, D. M. Minic, U. Van Kolck, and R. Vega, Phys. Lett. **B284** (1992) 384.
- [93] H. Yukawa, Proc. Phys. Math. Soc. Japan **17** (1935) 48.
- [94] J. L. Gammel and R. M. Thaler, Phys. Rev. **107** (1957) 291.
- [95] F. Myhrer and J. Wroldsen, Rev. Mod. Phys. **60** (1988) 629.
- [96] L. Ya. Glozman, Nuc. Phys. **A663/664** (2000) 103c.
- [97] D. Bartz and Fl. Stancu, Phys. Rev. **C63** (2001) 034001.
- [98] M. L. Goldberger and S. B. Treiman, Phys Rev. **111** (1958) 354.
- [99] T. E. O. Ericson, B. Loiseau, and A. W. Thomas, hep-ph/0009312 (2000).
- [100] V. Bernard, N. Kaiser and U. G. Meissner, Phys. Rev. **D50** (1994) 6899.
- [101] A. Manohar and H. Georgi, Nucl. Phys. **B234** (1984) 189.
- [102] J. Botts et al., Phys. Lett. **B304** (1993) 159.
- [103] A. D. Martin, R. G. Roberts, and W.J. Stirling Phys. Lett. **B308** (1993) 377.
- [104] R. G. Sachs, Phys. Rev. **126** (1962) 2256.
- [105] N. Isgur, Phys. Rev. Lett. **83** (1999) 272.
- [106] R. Carlitz, S. D. Ellis, and R. Savit, Phys. Letts **B64** (1976) 85.
- [107] N. Isgur, G. Karl, and D. W. L. Sprung, Phys. Rev. **D23** (1981) 163.

- [108] W. Melnitchouk, hep-ph/9909463 (1999).
- [109] B. Kubis and U. G. Meissner, Nucl. Phys. **A679** (2001) 698; and references therein.
- [110] A. W. Thomas, Phys. Lett. **B126** (1983) 97.
- [111] J. D. Sullivan, Phys. Rev. **D5** (1972) 1732.
- [112] S. Kumano, Phys. Rep. **303** (1998) 183.
- [113] J. P. Speth and A. W. Thomas, Adv. Nucl. Phys. **24** (1998) 83.
- [114] E. M. Henley and G. A. Miller, Phys. Lett. **251** (1990) 453.
- [115] S. Kumano, Phys. Rev. **D43** (1991) 3067; **D43** (1991) 59; S. Kumano and J. T. Londergan, Phys. Rev. **D44** (1991) 717.
- [116] A. Signal, A. W. Schreiber, and A. W. Thomas, Mod. Phys. Lett. **A6** (1991) 271.
- [117] W. P. Hwang, J. Speth and G. E. Brown, Z. Phys. **A339** (1991) 383.
- [118] A. Szczurek, J. Speth and G. T. Garvey, Nucl. Phys. **A570** (1994) 765.
- [119] W. Koepf, L. L. Frankfurt and M. Strikman, Phys. Rev. **D53** (1996) 2586.
- [120] W. Melnitchouk, J. Speth and A. W. Thomas, Phys. Rev. **D59** (1999) 014033.
- [121] H. Holtzman, A. Szczurek and J. Speth, Nucl. Phys. **A596** (1996) 631.
- [122] N. N. Nikolaev, W. Schaefer, A. Szczurek and J. Speth, Phys. Rev. **D60** (1999) 014004.
- [123] A.W. Thomas, W. Melnitchouk, and F.M. Steffens, Phys. Rev. Lett. **85** (2000) 2892.
- [124] J. Gasser and H. Leutwyler, Ann. Phys. **158** (1984) 142.
- [125] S. Weinberg, Phys. Rev. Lett. **67** (1991) 3473.
- [126] T. P. Cheng and L. F. Li, Phys. Rev. Lett. **74** (1995) 2872.
- [127] T. P. Cheng and L. F. Li, Phys. Lett. **B366** (1996) 365.
- [128] K. Suzuki and W. Weise, Nucl. Phys. **A634** (1998) 141.
- [129] A. Szczurek, A. Buchmans and A. Faessler, J. Phys. **C22** (1996) 1741.
- [130] X. Song, J. S. McCarthy and H. J. Weber, Phys. Rev. **D55** (1997) 2624.
- [131] T. Ohlsson and H. Snellman, Eur. Phys. J. **C7** (1999) 501.
- [132] J. D. Bjorken, SLAC-PUB-5608 (1991).
- [133] T. P. Cheng and L. F. Li, Phys. Rev. **D57** (1998) 344.
- [134] T. P. Cheng and L. F. Li, hep-ph/9811279 (1998).
- [135] T. P. Cheng and L. F. Li, Phys. Rev. **D59** (1999) 097503.
- [136] T. P. Cheng, N. I. Kochelev and V. Vento, Mod. Phys. Lett. **A14** (1999) 205.
- [137] E. M. Henley, T. Renk and W. Weise, Phys. Lett. **B502** (2001) 99.
- [138] G. Piller and W. Weise, Phys. Reports **330** (2000) 1.
- [139] M. Vanttinen et al., Eur. Phys. J. **A3** (1998) 351; P. Hoyer and M. Vanttinen, Z. Phys. **C74** (1997) 113.
- [140] A. A. Belavin et al., Phys. Lett. **B59** (1975) 85.
- [141] G. t'Hooft, Phys. Rev. Lett. **37** (1976) 8.
- [142] T. Schaefer and E. Shuryak, Rev. Mod. Phys. **70** (1998) 323.
- [143] S. Forte, Phys. Lett. **B224** (1989) 189.
- [144] S. Forte, Acta Phys. Polon. **B22** (1991) 1065.
- [145] A. E. Dorokhov and N. I. Kochelev, Phys. Lett. **B259** (1991) 335; **B335** (1993) 167.
- [146] D. I. Diakonov et al., Nucl. Phys. **B480** (1996) 341.

- [147] K. F. Liu and S. J. Dong, Phys. Rev. Lett. **72** (1994) 1790.
- [148] K. F. Liu, Phys. Rev. **D62** (2000) 074501.
- [149] D. I. Diakonov et al., Phys. Rev. **D56** (1997) 4069.
- [150] P. V. Pobylitsa and M. V. Polyakov, Phys. Lett. **B389** (1996) 350.
- [151] P. V. Pobylitsa et al., Phys. Rev. **D59** (1999) 034024.
- [152] M. Wakamatsu and T. Kubota, Phys. Rev. **D57** (1998) 5755.
- [153] B. Dressler et al., hep-ph/9809487 (1998).
- [154] A. I. Signal and A. W. Thomas, Phys. Lett. **B191** (1987) 205.
- [155] M. Burkardt and B. J. Warr, Phys. Rev. **D45** (1992) 958.
- [156] X. D. Ji and J. Tang, Phys. Lett. **B362** (1995) 182.
- [157] S. Brodsky and B-Q. Ma, Phys. Lett. **B381** (1996) 317.
- [158] A. O. Bazarko et al., Z. Phys. **C65** (1995) 189.
- [159] D. Kaplan and A. Manohar, Nucl. Phys. **B310** (1988) 527.
- [160] G. Garvey, W. Louis and H. White, Phys. Rev. **C48** (1993) 761.
- [161] B. Mueller et al., Phys. Rev. Lett. **78** (1997) 3824.
- [162] K. Aniol et al., Phys. Rev. Lett. **82** (1999) 1096.
- [163] M. Alberg et al., Phys. Lett. **B389** (1996) 367.
- [164] M. Alberg, T. Falter and E. M. Henley, Nucl. Phys. **A644** (1998) 93.
- [165] JHF Project Office. *Proposal for Japan Hadron Facility*, KEK Rep. **97-3** (1997).
- [166] C. N. Brown, unpublished (1998).
- [167] J. C. Peng et al., hep-ph/0007341 (2000).
- [168] D. Geesaman et al., *Fermilab proposal P906* (1999).
- [169] B-Q. Ma, Phys. Lett. **B274** (1992) 111.
- [170] J. T. Londergan and A. W. Thomas, *Progress in Particle and Nuclear Physics*, **41** (1998) 49.
- [171] C. Boros, J. T. Londergan and A. W. Thomas, Phys. Rev. Lett. **81** (1998) 4075; Phys. Rev. **D59** (1999) 074021.
- [172] J. C. Peng and D. M. Jansen, Phys. Lett. B **354** (1995) 460.
- [173] A. D. Martin, W. J. Stirling and R. G. Roberts, Phys. Lett. B **306** (1993) 145.
- [174] G. Bunce et al. Part. World **3** (1992) 1.
- [175] J. M. Moss, *Int. Conf. Polarization Phenomena in Nucl. Phys., AIP Conf. Proc.* **339** (1994) 721.
- [176] P. L. McGaughey, J. M. Moss and J. C. Peng, Annu. Rev. Nucl. Part. Sci. **49** (1999) 217.
- [177] C. Bourrely and J. Soffer Phys. Lett. **B314** (1993) 132.
- [178] B. Dressler, K. Goeke, M. V. Polyakov and C. Weiss, Eur. Phys. J. **C14** (2000) 147.
- [179] R. J. Fries and A. Schäfer, Phys. Lett. **B443** (1998) 40.
- [180] K. G. Boreskov and A. B. Kaidalov, Eur. Phys. J. **C10** (1999) 143.
- [181] B. Dressler et al., Eur. Phys. J. **C18** (2001) 719.
- [182] C. Adloff et al., Eur. Phys. J. **C6** (1999) 587.
- [183] J. C. Peng, Proceedings of the Second Workshop on Physics with a Polarized-Electron Light-ion Collider, Cambridge, MA, September, 2000.